CHAPTER
41

BWR REACTOR INTERNALS AND OTHER BWR ISSUES

Hardayal S. Mehta

41.1 INTRODUCTION

The objective of this Chapter is to provide some details of many and sometimes unique ways in which the provisions of Section III and Section XI have been used in addressing the service-induced degradations in the BWR vessels, internals, and pressure boundary piping. Among the items covered are reactor internals, weld overlays, and reactor vessel. The most common form of service-induced cracking in the stainless steel and Ni-Cr-Fe components in the BWR pressure boundary is typically due to intergranular stress corrosion cracking (IGSCC).

41.2 BWR INTERNALS

The BWR reactor internals fall into two categories. The first category includes components constituting the core support structure that are important to safe shutdown of the reactor. The components in this category include the shroud, shroud support structure, core plate, jet pumps, and such. Most of the BWR internals were designed using the guidance of Class 1 component design by analysis rules of Subsection NB in Section III. Only in some of the newer BWRs was Subsection NG formally used. The second category includes internal components (e.g., steam dryer) that are not safety related (i.e., not important to safe shutdown of the reactor). Only some recently observed cracking in steam dryers under increased steam flows due to extended power uprate has drawn some attention to the need for inspection and detailed stress evaluation of this component to assure its structural integrity [1]. The discussion in this section is mostly focused on the first category of components; the steam dryer issues are covered at the end of this section. Figure 41.1 shows a schematic of the BWR internal components.

Most of the BWR RPV internals are fabricated from either stainless steel or Ni-Cr-Fe to avoid the presence of corrosion products in the reactor water. In view of the earlier IGSCC experience with Type 304 and 316 stainless steels in external piping, the material for later-constructed BWR internals was replaced by lower carbon (L grade, carbon $<0.035\%$) stainless steels [2,3]. For some of the replacement external piping, low carbon stainless steel with added nitrogen (LN grade) for structural strength (i.e., higher S_m value) was used. An additional degradation mechanism for the reactor internals is the irradiation. The irradiation can cause the initiation of cracking (irradiation-assisted stress-corrosion cracking or IASCC), accelerated crack growth rate, and a reduction in fracture toughness. Typically, the components affected by irradiation are the shroud and the top guide.

41.2.1 Inspection, Evaluation, and Repair Methods

In the Section XI space, the reactor internals fall under category B-N-2 core support structures. However, Section XI does not have evaluation standards or repair/replacement guidelines available for this category for the following reason [4]: "A Subgroup of SC XI was established to develop a complete program, including evaluation standards and repair/replacement techniques. After several years of work to establish generic requirements and, later, to separate PWR and BWR requirements, the Subcommittee failed to reach a consensus on its approach, and because industry interest and support had diminished, the effort was terminated. The power plants and the NRC now resolve problems on an individual basis."

In the wake of the observed cracking in the shroud of an overseas reactor followed by several in the United States, an urgent need was identified to develop inspection, evaluation, and, if necessary, repair techniques. The BWR Vessels and Internals Project (BWRVIP) was formed in 1994 with the following objectives [5–7]: to lead the BWR industry towards generic resolution of reactor pressure vessel and internals materials condition issues; to identify or develop generic cost-effective material management strategies from which each operating plant will select the most appropriate alternative; to serve as the focal point for the regulatory interface with the industry on BWR vessel and internals issues; and to share information and promote communication and cooperation among participating utilities. The first BWR internal component addressed was the shroud. Since then, over 100 reports have been published by the BWRVIP on the various internals and RPV issues. Key reports have been approved by the NRC for use by utilities on a generic basis. This obviates the need for an individual submittal and its review/approval by the NRC for a specific technical evaluation. Most of the BWRVIP reports are proprietary. However, technical details from the published technical papers are provided in this Section to illustrate the use of flaw evaluation procedures of IWB-3600 in flaw disposition.

41.2.2 Shroud

One of the first BWR internal components to show cracking was the shroud, and the observed cracking was in the heat-affected

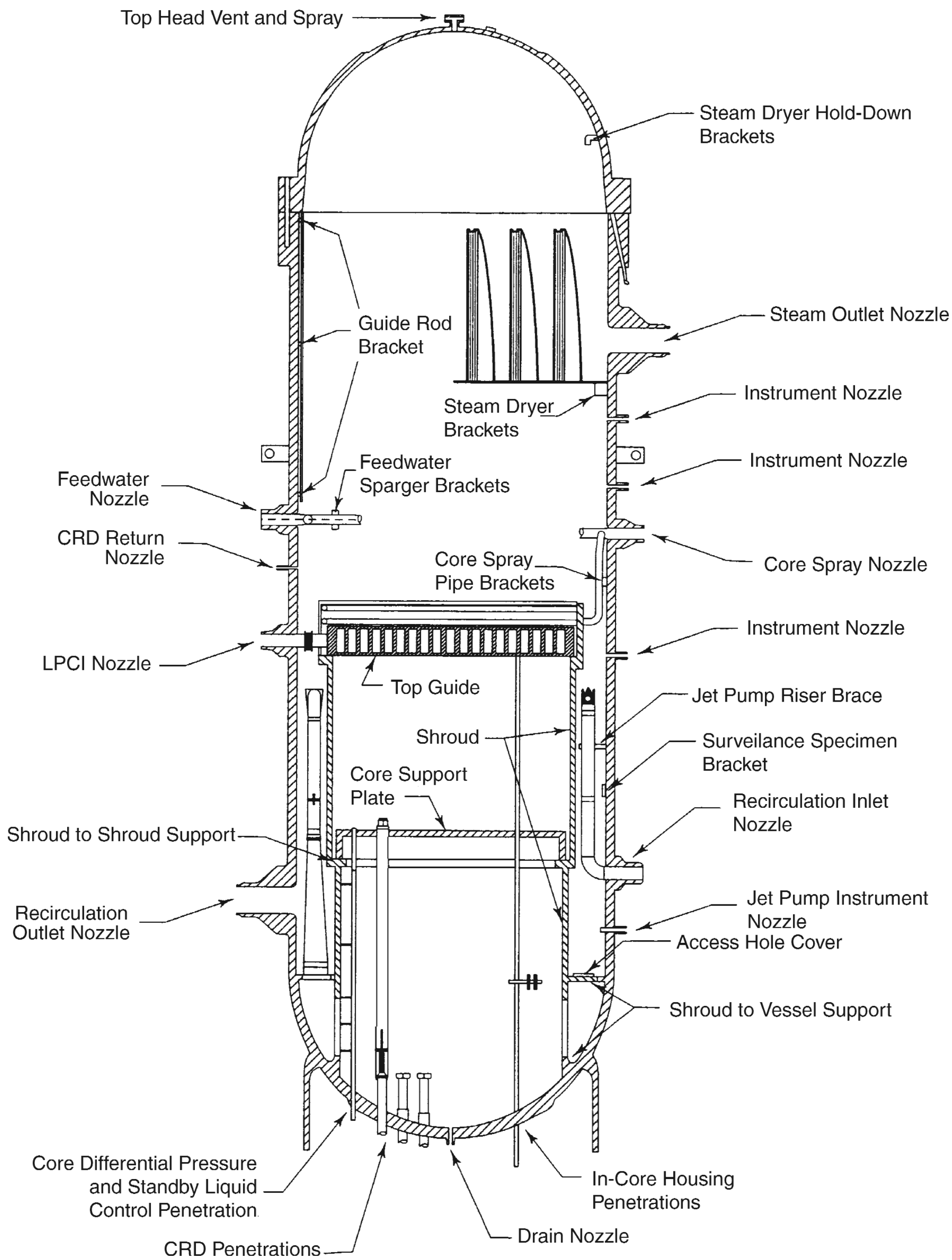

FIG. 41.1 OVERVIEW OF BWR PRESSURE VESSEL AND INTERNAL COMPONENTS

zones (HAZs) of the circumferential welds. The BWR shroud is a cylindrical structure surrounding the core. The shroud material is Type 304 or 304L grade stainless steel. It is typically 200 in. in diameter and 1.5–2 in. thick. It is constructed by welding together several cylindrical sections (see Fig. 41.2).

The limit load methodology for cylindrical geometries outlined in Appendix C of Section XI has been used as a flaw evaluation guideline for the shroud [8]. However, several additional considerations were required to complete an analytical evaluation of flaws per IWB-3600. These considerations include crack growth rate under BWR water environment, inspection uncertainty, and the fracture toughness considering irradiation effects.

41.2.2.1 SCC Growth Rate Relationships. The crack growth rate relationship for stainless steels included in the current Section XI is for fatigue mechanism in air environment only. For a crack exposed to BWR water environment, the crack growth rate due to stress corrosion cracking (SCC) essentially overwhelms that due to fatigue. The Section XI Committee is currently in the process of developing SCC growth rate relationships for austenitic materials.

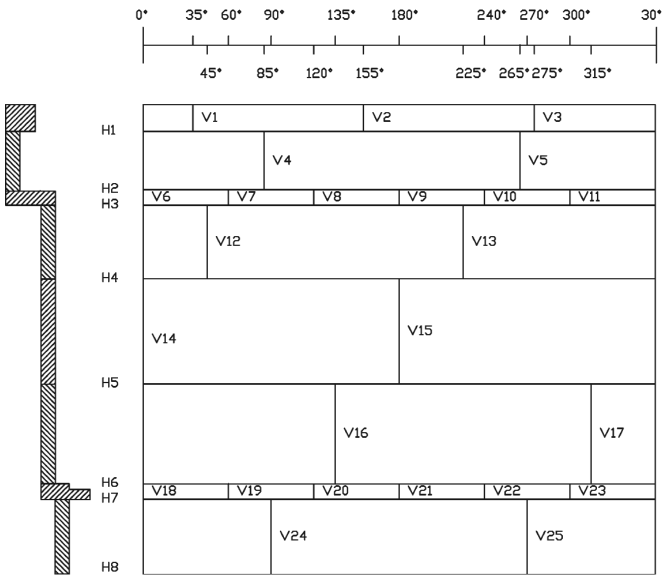

FIG. 41.2 BWR CORE SHROUD WELD DESIGNATIONS

In the crack length direction, the evaluations use a bounding crack growth rate of 5×10^{-5} in./hr approved by the USNRC [9,10].

The detailed guidance for the crack growth rates (CGRs) used in the evaluation of BWR stainless steel internals is provided in BWRVIP-14 [11], as modified by the stipulations given in the NRC's final safety evaluation (SE) [12] on this report. The SE stated, in part, ". . . by using an appropriately reduced value for the CGR from the 5×10^{-5} in./hr value found in NUREG-0313, Rev. 2, it would be possible for licensees to get credit for improved water chemistry and other measures to mitigate cracking, e.g., hydrogen water chemistries (HWC) and/or noble metal additions. The revised CGR of 2.2×10^{-5} in./hr corresponds to water chemistries with a conductivity of ≤ 0.15 μS/cm and an electrochemical potential (ECP) of $+200$ mV. The BWRVIP-14 correlation indicates that this bounding CGR could be reduced for HWC with ECP ≤ -230 mV. The staff finds acceptable a reduction in the CGR from 2.2×10^{-5} in./hr to 1.1×10^{-5} in./hr for plants with HWC. The crack growth rates stated are only applicable to components with uences $< 5 \times 10^{20}$ n/cm^2 ($E > 1$ MeV), since the CGR database is presently based only on unirradiated materials."

In many of the inspected shrouds, the fluence at the midcore weld such as the H4 weld in Fig. 41.2 is greater than 5×10^{20} n/cm^2. For such cases, the approach used is to take no structural credit for the material that is expected to exceed the preceding value during the evaluation period [13]. The BWRVIP proposed SCC growth rate relationships [14] are currently under review by the NRC.

41.2.2.2 Inspection Uncertainty. The shroud inspections are typically conducted by either the visual testing (VT) or ultrasonic testing (UT) means. Since the VT cannot provide the crack depth, the VT-detected flaws are assumed as through-wall for the purposes of the shroud structural evaluation. The indication length and/or depth measurement uncertainties are a function of NDE delivery system that may vary by the vendor. The BWRVIP conducted an extensive program to document these uncertainties as a function of internal component, NDE method, vendor, and other variables [15]. For example, in one typical case [13], each nominally reported indication length and depth in the shroud was increased by 0.472 in. and 0.108 in., respectively, for the purpose of the structural evaluation.

41.2.2.3 Irradiated Stainless Steel Fracture Toughness. Data showing trends in yield strength, reduction in area, and uniform elongation as a function of fluence at irradiation and test temperature of 550°F have been published previously [16,17]. A review of this data indicated that the yield strength increases occur at a significant rate beyond $3 - 5 \times 10^{20}$ n/cm^2. Based on this and other ductility data, the limit load flaw evaluation for the shroud is also supplemented by a LEFM/EPFM analysis where the fluence exceeds 3×10^{20} n/cm^2. Based on the irradiated fracture toughness tests reported [18−20], a K_{Ic} value of 150 ksi $\sqrt{\text{in.}}$ has been used in the shroud flaw evaluations [15]. Additional irradiated stainless steel fracture toughness data in the fluence range of BWR shrouds have also recently become available [21]. The BWRVIP has developed fracture toughness relationships for irradiation levels covering fluences in excess of 1×10^{21} n/cm^2 [22] that have been reviewed and approved by the NRC.

41.2.2.4 Evaluation With Multiple Indications. When multiple indications are involved, which is generally the case, a conservative approach is to stack all of the indications (after adding crack growth, inspection uncertainty, and the application of proximity criteria) into one continuous flaw and compare it with the allowable flaw length calculated using the limit load equation of Appendix C. However, this approach is too conservative and, therefore, an alternative approach has generally been followed.

Figure 41.3 shows a schematic representative plan view of an asymmetrically distributed uncracked ligament. It is assumed that there are 1, 2,...i,...n ligament lengths and that the i length is of thickness t_i and extends from an azimuth of θ_{i1} to θ_{i2}. The ligament length li of the i ligament is related to azimuth angles θ_{i1} and θ_{i2} by the following relationship:

$$l_i = (D/2)(\theta_{i1} - \theta_{i2}) \tag{1}$$

where

D = the diameter of the shroud

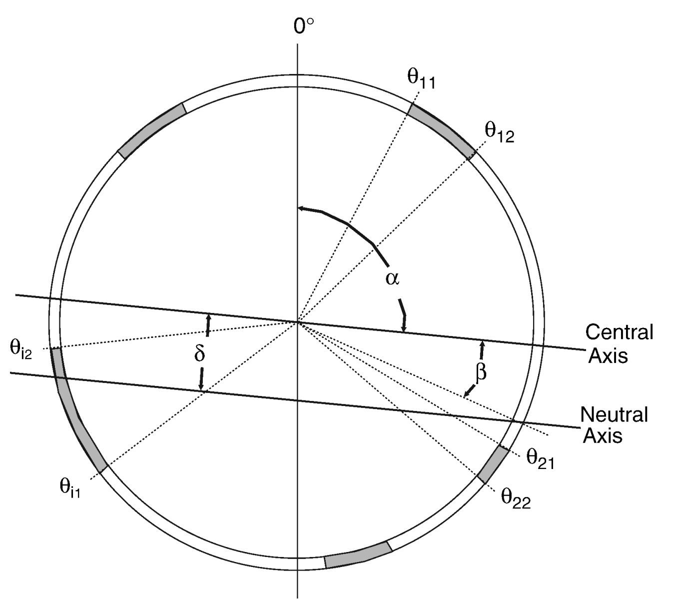

FIG. 41.3 A DISTRIBUTED LIGAMENT LENGTH EXAMPLE

The calculation of moment M that this ligament configuration can resist is somewhat complicated, because it is not a priori clear as to which azimuthal orientation of the neutral/central axis would produce the least value of bending moment, M. Therefore, the value of M is calculated for various orientations of the central axis from 0° to 360°. This calculation is performed in the following two steps:

(a) In this step, a central axis orientation, α is first selected. The location of the neutral axis, which is parallel to the central axis, at a distance δ from the central axis is determined using the following (see Fig. 41.3):

$$\int_{-(\pi-\alpha+\beta)}^{\alpha+\beta} Rt(\theta)\, d\theta - \int_{\alpha+\beta}^{-(\pi-\alpha+\beta)} Rt_n\, d\theta = (\sigma_m/\sigma_f)(2\pi R t_n) \quad (2)$$

where

α = assumed azimuth angle of the central axis
β = angle of the neutral axis with respect to central axis, or $\sin^{-1}(\delta/R)$
δ = distance between the central axis and the neutral axis
R = mean radius of the shroud
$t(\theta) = t_i$ (thickness of the i ligament), if angle θ is such that $\theta_{i1} < \theta < \theta_{i2}$, or 0 otherwise
t_n = nominal thickness of shroud
σ_m = membrane stress
σ_f = material flow stress = $3S_m$

Thus, this step helps define the location of the neutral axis when the central axis is assumed to be at an azimuth angle of α.

(b) Once the location of the neutral axis relative to the central axis is determined, the moment $M\alpha$ is then obtained by integrating the bending moment contributions from individual ligament lengths. The mathematical expression used is the following:

$$M_\alpha = \int_{-(\pi-\alpha+\beta)}^{\alpha+\beta} \sigma_f R^2 t(\theta) \sin(\alpha-\theta)\, d\theta - \int_{\alpha+\beta}^{-(\pi-\alpha+\beta)} \sigma_f R^2 t_n \sin(\alpha-\theta)\, d\theta \quad (3)$$

The orientation α that produces the least value of M is called α *min* and defines the axis capable of resisting the limiting moment. Whether the specified set of uncraked ligament lengths provides the required structural margin is verified by the following:

$$M_{\alpha\, min}/Z + P_m \geq SF(P_m + P_b) \quad (4)$$

where

Z = section modulus of the shroud based on uncracked cross-section
P_m = applied membrane stress
P_b = applied bending stress
SF = safety factor

The current approach uses a safety factor of 2.78 for normal/upset (Level A/B) conditions and 1.39 for emergency/faulted (Level C/D) conditions.

41.2.2.5 Repair/Replacement. BWR utilities have taken a variety of approaches to addressing shroud cracking, ranging from a proactive implementation of a preemptive repair to an inspection based approach in which a repair is installed only when warranted by periodic inspection results. The approach selected by a utility is based on many factors, including a plant-specific assessment of the potential for significant cracking. The design, fabrication, and installation of a shroud repair implemented at a BWR plant has been described [23]. An example of the shroud replacement (along with other internals such as jet pumps) has been given [24]. The replacement shroud material was chosen as Type 316L stainless steel to ensure higher IGSCC resistance.

41.2.3 Jet Pumps

The jet pump recirculation system provides forced circulation flow through the BWR core. During the normal operation of the plant, the jet pump structure is subjected to flow-induced vibration (FIV) and exposed to a high-temperature (approximately 530°F) reactor water environment. The FIV loading could produce fatigue crack growth in a flaw if the applied stress intensity factor range exceeds the fatigue threshold (cyclic stress intensity factor range, ΔK_{th}) below which cracks do not propagate (i.e., virtually no crack growth) under cyclic stress. The magnitude of the FIV stresses is proportional to the square of the flow rate in the riser. The power produced by the reactor is typically proportional to the core flow rate. Thus, the predicted fatigue crack growth at a flaw would depend on the operating scenario (i.e., core flow) assumed.

An example of the flaw evaluation at one of the locations in a jet pump where inservice inspection (ISI) detected an indication has been provided [25]. The flaw was approximately 13 in. long, oriented circumferentially, and located in a 10-in. diameter schedule 40 section. Figure 41.4 shows the BWR jet pump geometry. For the analysis purposes, the flaw was assumed to be through-wall. Since it is not a pressure boundary, a through-wall flaw in a reactor internal is acceptable for continued operation as long as the safety margins of either the original Code of construction or ASME BPVC Section XI are satisfied. Allowable circumferential flaw length was determined as approximately 18 in. using the limit load equations (with a/t assumed to be 1.0) in Appendix C of Section XI. The SCC growth rate was assumed to be 5×10^{-5} in./hr.

The flaw length at inspection was such that crack growth due to fatigue during next cycle of operation could not be ruled out. A key input in the fatigue crack growth evaluation was the relationship between the applied stress intensity range (ΔK) and the crack growth rate per cycle (da/dN). The fatigue crack propagation behavior above ΔK_{th} can be represented by the following equation:

$$da/dN = C(\Delta K)^n \quad (5)$$

where

da = increment in crack length, a
N = number of cycles
ΔK = mode I stress intensity factor range(C and n are constants)

The ΔK is equal to the maximum value of K (K_{max}) minus the minimum value of K (K_{min}). When a mean stress or load is present, the value of K_{min} is different from the negative of K_{max}. An indication of the relative magnitudes of the mean and the fluctuating stresses is the R ratio or R, defined as K_{min}/K_{max}. The cyclic frequency of the FIV stresses is on the order of 32 Hertz. This cyclic frequency is high enough that the reactor water environmental

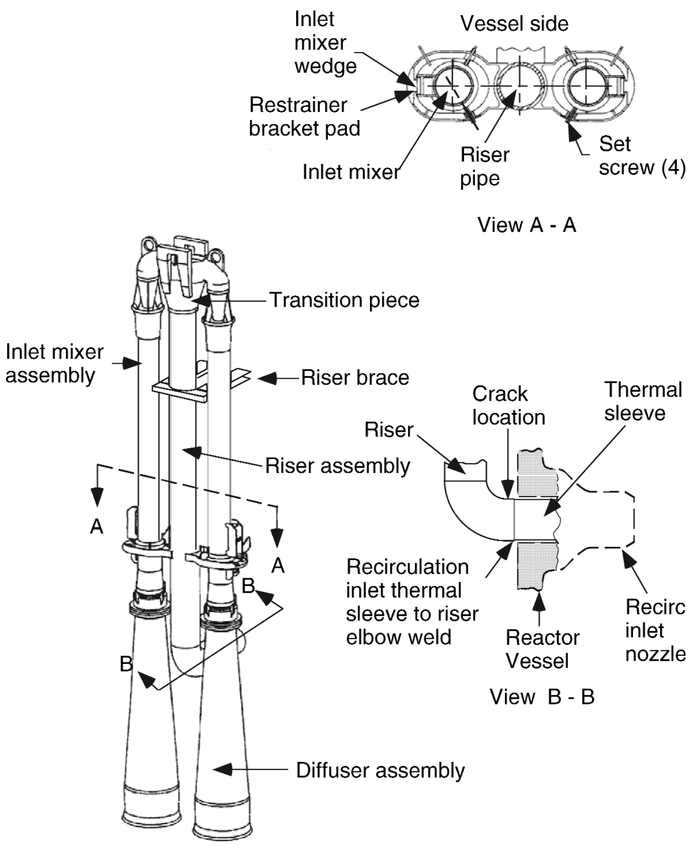

FIG. 41.4 TYPICAL GEOMETRY OF A BWR JET PUMP

effects are expected to be negligible. Therefore, the fatigue crack growth rate relationship developed in air environment was used in the evaluation. ASME Section XI, Fig. C-3210-1 of Appendix C shows air fatigue crack growth rate curves for austenitic stainless steels. The exponent n of the curve is given as 3.3. The dotted-line curves in this figure are at 550°F. The R ratio for the subject flaw configurations was determined to be of the order of 0.5. Interpolation between R values of 0.0 and 0.79 was used to obtain the curve for $R = 0.5$.

A review of the GE test data [26] and those available in the open literature indicated that 5 ksi$\surd\sqrt{\text{in.}}$ is a reasonably conservative value for K_{th} at $R = 0.5$. Thus,
the fatigue crack growth rate relationship used in this evaluation was mathematically represented as the following:

$$da/dN = 2.705 \times 10^{-10} (\Delta K)^{3.3} \quad \text{for} \quad \Delta K \geq 5 \text{ ksi}\sqrt{\text{in.}} \qquad (6)$$
$$= 0.0 \quad \text{for} \quad \Delta K < 5 \text{ ksi}\sqrt{\text{in.}}$$

During startup testing, the riser brace is instrumented with strain gages and, thus, the strain/stress ranges at that location are available. The key task is to infer the stress-time history at the cracked location given the stress-time history at the riser brace. The steps involved in calculating the vibration stress ranges at the cracked section from the test data are summarized as follows:

(a) Review the startup vibration data for the applicable lead plant to determine the primary structural modes of interest for the jet pump. A 128-sec trace of the startup test data was available for this purpose.
(b) Using a finite element model of the jet pump, determine the natural frequencies, mode shapes, and modal stresses of all structural modes of interest. Compare the results to the startup test results to ensure applicability of strain measurements.
(c) From the modal stresses, determine the mode shape factor for each mode of interest to relate the strain at the riser brace to the stress at the crack location.
(d) Decompose the riser brace strain-time history into individual modal strain-time histories for each mode of interest. The jet pump riser brace-time history is from the startup test data for the lead plant, whose jet pump was identical in design to that for the plant with cracked thermal sleeve.
(e) Multiply these individual modal strain-time histories by their corresponding mode shape factors to arrive at the crack location modal stress–time histories.
(f) Algebraically sum (recombine) the modal stress–time histories at the crack location to arrive at the resultant stress–time history. Care was taken in the decomposition (d) and recombination processes to ensure that the phase relationships among the modal components were maintained. Figure 41.5 shows the plot of a small segment of the stress-time history.
(g) Using the resultant stress-time history at the crack location, rank the stress amplitudes from maximum to minimum.
(h) Combine the largest positive and negative amplitudes to determine the maximum stress ranges.
(i) Group the stress ranges in increments of 50 psi and count the number of cycles in each group. Assign the median stress value to that group. For example, the cycles grouped in the 700–750 psi range were assigned a stress range of 725 psi.
(j) Scale the cycle numbers from the 128-sec test data sample to equivalent numbers for 100 hr of operation. The 100-hr interval was chosen to correspond to the time increment used in the crack growth calculation to update the crack length. Table 41.1 shows the resulting cycle numbers for each stress range determined.
(k) The ΔK values from the FIV stress cycles were determined using the mathematical expressions provided by Zahoor [27].

When the calculated value of ΔK for an FIV stress cycle exceeds the assumed threshold value of 5 ksi $\sqrt{\text{in.}}$, crack growth due to fatigue is predicted. Because the subject crack is also expected to experience crack growth due to SCC, the crack growth due to both mechanisms was linearly added. A small time interval of 100 hr was chosen to calculate the SCC and fatigue crack growth. The calculated value of crack growth from these two mechanisms was then added together and the crack length a at the beginning of the interval was updated to $a + 2\Delta a$. The factor of 2 accounts for crack growth at each end of the postulated

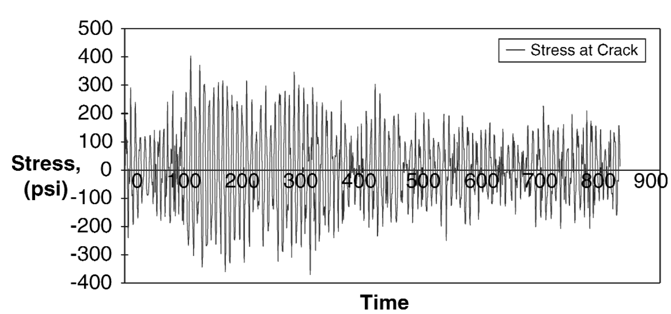

FIG. 41.5 SAMPLE OF STRESS TIME HISTORY AT CRACKED LOCATION

TABLE 41.1 JET PUMP FIV STRESS RANGE VERSUS CYCLE DATA (100 HR OF OPERATION)

Stress Range (psi)	Cycles
775	19,688
725	30,938
675	50,625
625	106,875
575	194,063
525	360,000
475	556,875
425	843,750

through-wall indication. This time-integration process was continued for operation intervals of interest.

Figure 41.6 shows the results of crack growth calculations for two core flow scenarios. The FIV stresses are proportional to the square of the core flow and, thus, the fatigue crack growth is sensitive to the assumed core flow. Typically, the power produced by the plant is directly proportional to core flow. At 80% core flow, the crack is predicted to grow to allowable crack length in 2,000 hours (~3 months) of operation. On the other hand, at 80% core flow level, the crack is predicted to grow to allowable value in excess of 8,000 hours or approximately 1 year of operation. The difference between the two scenarios is essentially the crack growth rate difference due to fatigue. Similar curves were generated for other core flow levels for use by the plant operator; this allowed for flexibility in operating at different core flow (power) levels while ensuring that predicted total crack length is less than the allowable value.

Following approximately 4 months of operation at 80% core flow, the plant was shut down for the installation of repair hardware at the cracked weld. UT ultrasonic examination of the crack prior to the installation of the repair showed virtually no crack growth since the last examination. This confirmed the conservative nature of the fracture mechanics and crack growth evaluations to justify continued operation in the as-is condition for a limited period. The repair consisted of installing a tongue-and-groove type of clamp to replace the cracked weld.

41.2.4 Other BWR Internals and Steam Dryers

Other internal components covered by the BWRVIP reports are core shroud support, top guide, core plate, core spray piping/spargers, standby liquid control system, CRD guide/stub tube/housing instrument penetrations, and vessel ID brackets. The flaw evaluation guidelines for most of these components are essentially based on the limit load methods described in Appendix C of ASME BPVC Section XI.

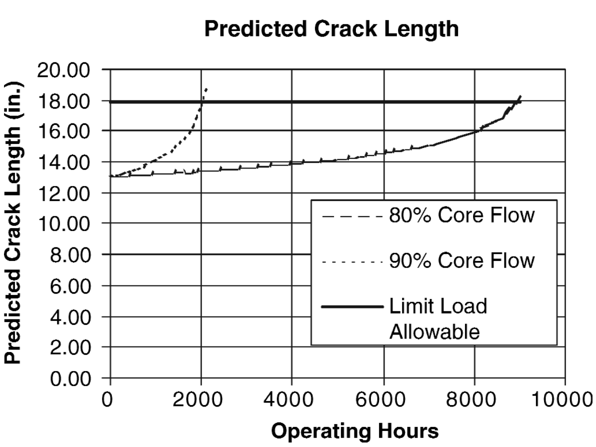

FIG. 41.6 PREDICTED CRACK LENGTHS FOR VARIOUS CORE FLOW LEVELS

Recently observed fatigue failure in the steam dryer of a BWR plant has focused attention on this component [1]. Although performing a nonsafety-related function, the steam dryer in a BWR plant must maintain its structural integrity to avoid loose dryer parts from entering the reactor vessel or steam lines and adversely affecting plant operation. Figure 41.7 shows the details of a BWR steam flow path and the steam dryer assembly. The steam dryer assembly is mounted in the reactor vessel above the steam separator assembly and forms the top and the sides of the wet steam plenum. Vertical guides on the inside of the vessel provide alignment for the dryer assembly during installation. The dryer assembly is supported by pads extending inward from the vessel wall. Steam from the separators flows upward and outward through the drying vanes. These vanes are attached to a top and bottom supporting member forming a rigid, integral unit. Moisture is removed and carried by a system of troughs and drains to the pool surrounding the separators and then into the recirculation down-comer annulus between the core shroud and RPV wall.

Figure 41.8 shows the failure locations in a steam dryer [28]. Extensive metallurgical and analytical evaluations (e.g., detailed finite element analyses, flow-induced vibration analyses, computational fluid dynamics analyses, 1:16 scale model testing, and acoustic circuit analyses) concluded that the root cause of this steam dryer failure was high cycle fatigue driven by flow-induced vibrations associated with the higher steam flows during extended power uprate (EPU) conditions (~18% above the original rated power). It is noted that no significant fatigue failures were observed in this dryer during the rated thermal power operation for more than 20 years. Most of the plant start-up FIV data are at the original rated power level or less, and the sensors, such as strain gages, on the dryer were not necessarily located where the fatigue failures were observed during EPU operation. The repairs at the failure locations were designed to provide a significant relative improvement (e.g., a factor of improvement in excess of 3) in the cyclic fatigue stress compared to that in the previous configuration. This technical approach was necessary in view of significant uncertainty in the fatigue loading during uprated condition operation. A recommended action was, among others, a VT-1 inspection of susceptible locations as determined by a dryer stress analysis [28]. Subsequently, the BWRVIP has developed an inspection and evaluation guidelines document [29] for the BWR steam dryers. The current stress analyses are conducted using the ASME BPVC Section III, Class 1 rules as guidance. Some of the activities currently in progress include extensive subscale model testing and acoustic circuit analysis. Also, some of the replacement steam dryers are being instrumented with strain gages and accelerometers to validate the analytically calculated vibratory stress magnitudes.

41.3 BWR PRESSURE VESSEL

41.3.1 Application of Probabilistic Fracture Mechanics for Inspection Exemption

The ISI of pressure-retaining RPV shell welds (Category B-A welds in Table IWB-2500-1) is an important element of ASME BPVC Section XI inspection requirements. Examination of the BWR vessel beltline region in early design BWRs posed problems

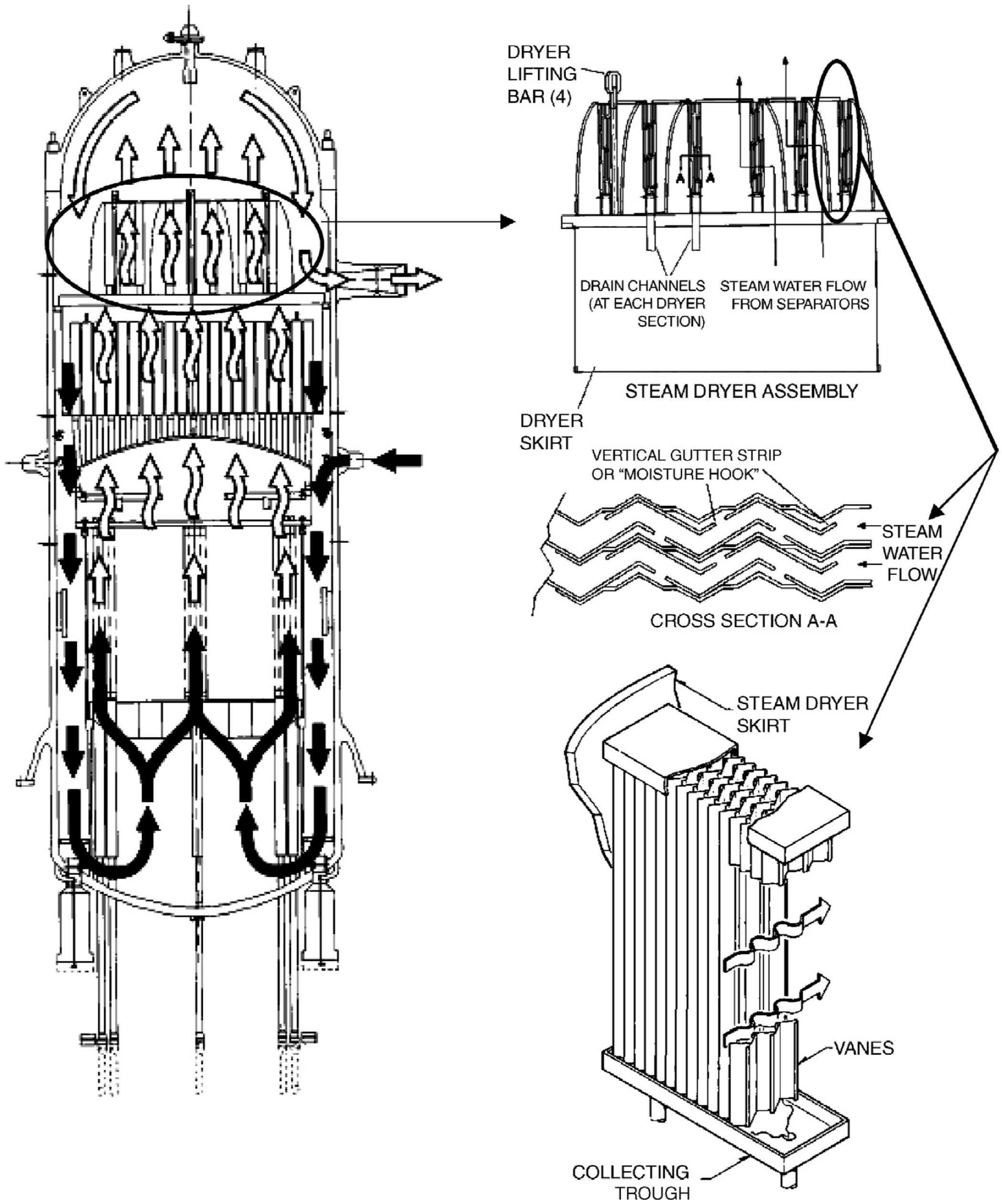

FIG. 41.7 BWR STEAM DRYER ASSEMBLY (WHITE ARROWS INDICATE STEAM FLOW PATH)

because of the limited access on the outside surface between the vessel and the biological shield. Also, interference from jet pumps and the complication of inspecting through the clad made inspection from the inside surface difficult. For the older plants with access problems, the NRC had granted exemption from the inspection requirement. In the early 1990s, the NRC changed its position and required inside diameter (ID) examinations of the older BWRs. This has led to the development of new inspection systems to meet the challenge of ID inspections [30]. Over the past several years, BWRVIP has developed [31] and successfully completed a program to assess the reliability of BWR vessels, specifically focusing on the effect of not inspecting the RPV circumferential welds [32]. The technical approach is based on probabilistic fracture mechanics (PFM) [33].

"In January 1991, the NRC published in the *Federal Register* a proposed Rule to amend Section 50.55a to Title 10 of the *Code of Federal Regulations* [10 CFR 50.55a], 'Code and Standards' [33]. One purpose of this amendment was to incorporate by reference a later edition and addendum to ASME BPVC Section XI, Division 1, and Addenda through 1988. Also, the rule proposed to create Section 50.55a(g)(6)(ii)(A) to 10 CFR 50.55a, "Augmented Examination of Reactor Vessel," which required that all licensees perform volumetric examinations of "essentially 100%" of the RPVs pressure-retaining shell welds during all inspection intervals in accordance with ASME BPVC Section XI on an "expedited" schedule, and revoked all previously granted reliefs for RPV weld examinations. Expedited in this context effectively meant during the inspection interval when the rule was approved or the first period of the next inspection interval. The final rule was published in the *Federal Register* on August 6, 1992.

By letter dated September 28, 1995, as supplemented, the BWRVIP submitted EPRI proprietary report BWRVIP-05 [31].

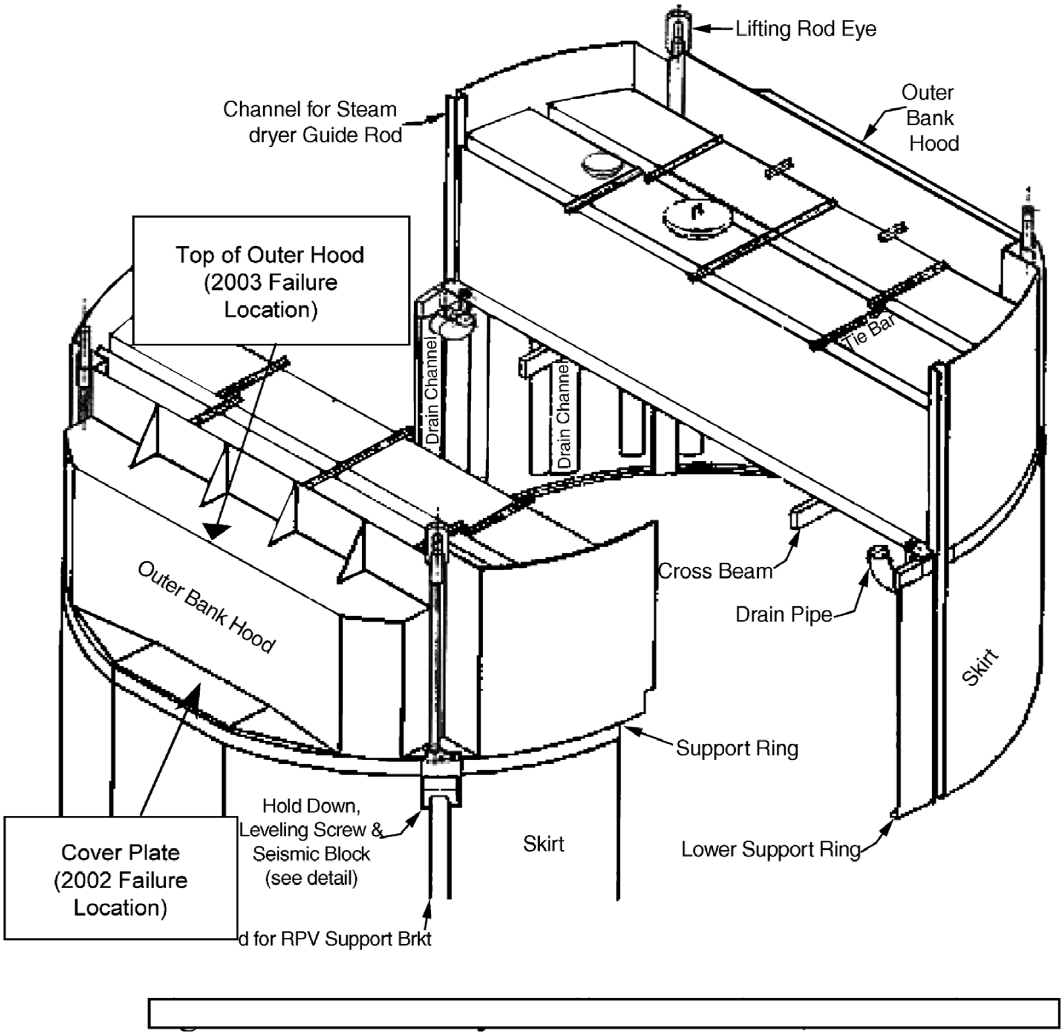

FIG. 41.8 STEAM DRYER DAMAGE

The BWRVIP-05 report evaluated the current inspection requirements for the RPV shell welds in BWRs, formulated recommendations for alternative inspection requirements, and provided a technical basis for these recommended requirements. As modified, it proposed to perform ISI on "essentially 100% of the RPV axial shell weld, and eliminate the inspection of all but approximately 2–3% of the circumferential welds at the intersection of the axial and circumferential welds."

The NRC's technical bases for granting this exemption are summarized. "Regulatory Guide 1.174 provides guidelines as to how defense-in-depth and safety margins are maintained, and states that a risk assessment should be used to address the principle that proposed increases in risk, and their cumulative effect, are small and do not cause the NRC Safety Goals to be exceeded. The estimated failure frequency of the BWR RPV circumferential welds is well below the acceptable core damage frequency (CDF) and large early release frequency (LERF) criteria discussed in RG 1.174. Although the frequency of RPV weld failure cannot be directly compared to the frequencies of core damage or large early release, the staff believes the estimated frequency of RPV circumferential weld failure bounds the corresponding CDF and LERF that may result from a vessel weld failure. On the above bases, the NRC staff concluded that the BWRVIP-05 proposal, as modified, to eliminate BWR vessel circumferential weld examinations, was acceptable."

The alternate PFM analysis of the NRC also considered a low-temperature overpressure (LTOP) transient at a non-U.S. BWR [34]. During this transient, the RPV was subjected to high pressure (7.9 MPa or 1,150 psig) at a low temperature (26–31°C or 79°–88°F). An Appendix E–based deterministic fracture mechanics analysis and corrective actions that justified plant startup following the transient are documented [34].

The PFM analysis can also be used to justify inspecting less than 100% of the vertical welds due to the local inaccessibility of the RPV and equipment issues. During a refueling outage, a U.S. BWR found that only 89.9% of the total length of the beltline vertical welds and 91.8% of the total vessel vertical weld length could be inspected. In the case of one particular vertical weld, the entire length was not accessible. Part of this weld was in the beltline region. A PFM evaluation [35] concluded that the resultant increase in the vessel failure probability was very small, even after factoring in the contribution of a postulated LTOP event. Thus, a less than 100% inspection of the welds was technically justified.

41.3.2 Feedwater Nozzle

Cracking was observed in BWR feedwater nozzles and control rod drive (CRD) return line nozzles during the 1970s. Since then, the CRD return lines in most BWRs have been rerouted and the

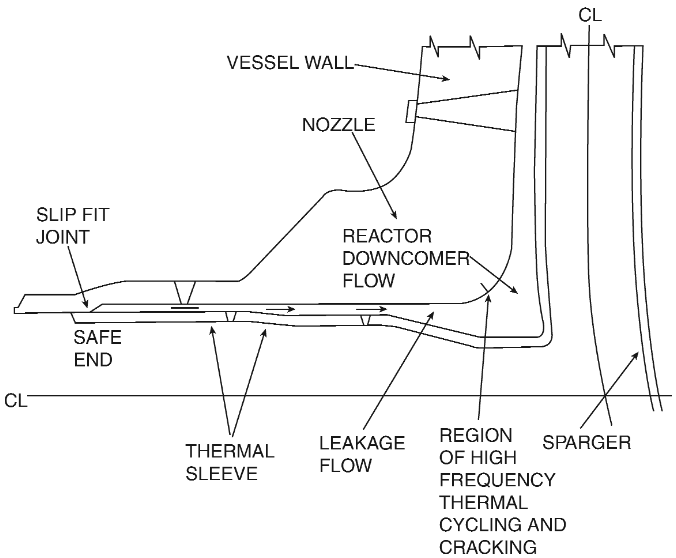

FIG. 41.9 CROSS-SECTION OF FEEDWATER NOZZLE WITH CRACKING LOCATION

nozzles capped. In the case of the feedwater nozzle, an extensive study of the problem attributed the cracking to relatively cooler feedwater leaking past loosely fitted sparger thermal sleeves installed inside the nozzle. The bypass leakage from around the loose thermal sleeves caused fluctuations in nozzle metal temperatures, which resulted in metal fatigue and crack initiation (see Fig. 41.9). These cracks were then driven deeper by the larger temperature and pressure cycles associated with startups, shutdowns, and certain operational transients. The NRC issued its findings and resolutions of the cracking problem in NUREG-0619 [36] in which it recommended that licensees take the following six actions to reduce the potential for initiating and growing cracks in the inner nozzle areas:

(a) remove the cladding from the inner radii
(b) replace loose-fitting or interference-fitting sparger thermal sleeves
(c) evaluate flow controllers for acceptability
(d) modify operating procedures to reduce thermal fluctuations
(e) reroute reactor water clean-up system to both feedwater loops
(f) conform to the inspection interval specified in Table 41.2 of NUREG-0619

Most of the BWRs adopted a triple thermal sleeve design as replacement for the original loose-fitting design. This design was developed as a part of an extensive experimental and analytical program [37] conducted to address feedwater nozzle cracking. Figure 41.5 shows this design and the temperature variations with and without bypass.

In 1981, the NRC issued Generic Letter 81-11 amending the recommendations in NUREG-0619. The generic letter allowed plant-specific fracture mechanics analysis in lieu of hardware modifications. To be acceptable to the NRC, such analysis had to analytically demonstrate that stresses from conservative controller temperature and flow profiles, when added to those resulting from the other crack growth phenomena such as startup/shutdown cycles, did not result in the growth of an assumed crack to greater than the allowable value of 1 in. during the 40-year life of the plant. The BWR feedwater nozzles have large flaw tolerance. The leak-before-break analyses concluded that even a through-wall flaw is structurally acceptable at the cracking location [37]. Thus, the critical flaw depth at this location is the through-wall dimension, typically 10 in. in most BWRs. If the approach of ASME BPVC IWB-3611 (for normal/upset conditions) is taken in setting the allowable flaw depth to be one-tenth of the critical flaw depth, one obtains the value of 1 in. as the allowable flaw depth.

The initial flaw depth is assumed to be 0.25 in.; this is considered to be a reasonable depth detectable with a high degree of confidence. The fatigue crack growth rate relationship used is that provided in Appendix A of ASME BPVC Section XI for water environment. This fracture mechanics analysis is essentially similar to a flaw tolerance evaluation per Appendix L of ASME BPVC Section XI. Figure 41.11 shows the results of fracture mechanics calculations for some of the BWRs. The results show a fairly large interval (in excess of 25 years) before the projected crack depth reaches 1 in.

Improvements in UT capability and the acceptable crack growth results seen in a majority of the fracture mechanics analyses provided justification to revise the inspection frequency and allow an alternate method. In fact, it was the intent of the NRC to eliminate penetrant testing (PT) requirements when improved UT techniques were available. The revised inspection schedules (see Table 41.2) were developed [38] and were approved by the NRC [39] for use by the BWR owners. The inspection zones referred to in Table 41.2 are shown in Fig. 41.12. The inspection intervals based on Table 41.2 provide considerable relief in inspection efforts without sacrificing safety.

Several BWR plants have implemented thermal sleeve bypass leakage detection systems since the time NUREG-0619 was published. Such systems were still under development at that time, but preliminary testing and implementation of the systems suggested them to be feasible and practical. The intent of these systems was to detect significant leakage through degraded thermal sleeve seals or cracks in thermal sleeve welds. This detection was accomplished by relating exterior surface metal temperatures (from newly installed thermocouples) to leakage flow. Leakage monitoring was expected to be a beneficial system to employ, because it might provide the most direct assessment of conditions known to lead to nozzle fatigue cracking.

Leakage monitoring systems have not been implemented as consistently as anticipated when NUREG-0619 was published. This has been primarily due to high installation and maintenance costs as well as field experience suggesting that the cracking problem had been eliminated. Also, erroneous leakage readings can be common with these systems due to sensor movement, which has led to unnecessary leakage concerns. Systems that have continued to operate properly have shown leakage to be insignificant; these results have further verified observations of no sparger cracking.

Based on these results, leakage monitoring does not possess the necessity and promise it once had. Nevertheless, for those installations that continue to operate properly, it does remain a viable method for further assessing the presence of fatigue cracking in nozzles. Therefore, for those plants that have such systems, leakage data obtained from these systems can be used to enhance the technical argument used to establish inspection frequency.

41.3.3 Inspections of Other Vessel Nozzles and Welds

41.3.3.1 Alternate Inspection Method for Nozzle Inner Radii. Other than the feedwater nozzles and the operational CRD

TABLE 41.2 FEEDWATER NOZZLE/SPARGER INSPECTION RECOMMENDATIONS(1)

Thermal Sleeve/Sparger Design Configuration	UT Inspection Interval Factor(2) for Zones 1 and 2 Method 1(3)	Method 2(3)	Methods 3 or 4(3)	Visual Inspection of Sparger(4)
Interference fit, clad nozzle	0.05	0.10	0.20	2
Welded, clad nozzle	0.10	0.17	0.33	2
Single thermal sleeve, single piston ring, unclad nozzle	0.10	0.17	0.33	4
Oyster Creek and Nine Mile Point 1 (unclad nozzle, significantly modified spargers installed)	0.10	0.17	0.33	4
Welded, unclad nozzle	0.10	0.17	0.33	4
Triple sleeve, double piston ring, unclad nozzle	0.10	0.17	0.33	4
Other Configurations	see note (5)	see note (5)	see note (5)	see note (5)

Notes: (1) The inspection interval is to begin at the time when a qualified inspection plan that meets the requirement of this report is established and implemented. The need for routine PT exams is eliminated.

(2) For each configuration, the maximum inspection interval is defined by a fraction of the time until a 0.25 inch or greater depth crack reaches the appropriate allowable value, as obtained from a plant-specific fracture mechanics analysis following the recommendations of Section 5.6 of this report. For example (when Method 3 is used):

Sparger Design = Triple Thermal Sleeve
Fracture Mechanics Result = 0.25″ crack grows to allowable depth in 30 years
Required UT Inspection Interval = Allowable time × Factor
= 30 × 0.33 = 10 years

For Zones 1 and 2, in no case shall the maximum allowable time between inspections exceed 10 years. For Zone 3, the inspection intervals can be twice the value recommended for Zones 1 and 2. The inspection frequency is not required to be more often then every second cycle regardless of interval factor.

(3) The UT methods are defined as follows:

Method 1 = Manual
Method 2 = Automated, Threshold Recording
Method 3 = Automated, Full RF Recording (No Threshold)
Method 4 = Phased Array (No Threshold)

(4) Visual inspection of flow holes and welds in sparger arms and sparger tees. These requirements are the same as those specified in NUREG-0619.

(5) Other configurations not specifically identified here should be evaluated on a case-by-case basis.

return line nozzles in BWRs, the ISI inspections of inner radii of the other RPV nozzles, including PWR vessel nozzles, have not found any indications. This led to the adoption of Code Case N-648-1 [40]. This Code Case allows a VT-1 examination of the inner radii surface [surface M-N in Figs. IWB-2500-7(a) through(d)] in lieu of the volumetric examination required by Table IWB-2500-1, Examination Category B-D, Item B3.20 or B3.100, for ISI of reactor vessel nozzles other than BWR feedwater nozzles and operational CRD return line nozzles. If crack-like surface flaws exceeding the acceptance criteria of Table IWB-3510-3 are found, acceptability for continued service can be shown by meeting the requirements of ASME BPVC IWB-3142.2, IWB-3142.3, or IWB-3142.4.

Briefly, the technical bases [41] for this Code Case are as follows: volumetric inspections have been required for the nozzle inner radius regions of reactor vessels since the inception of Section XI of the ASME Code in 1970. In over 30 years of inspections, no indications have been found in any pressurized water reactor (PWR) nozzles. Indications have been found in two nozzle types in boiling water reactor (BWR) nozzle, both the other nozzle types have the same flawless history as the PWRs. In 1999, a project was begun to eliminate this inspection from the requirements of ASME BPVC Section XI; the following three independent arguments were advanced:

(a) a good inspection history (the nozzles that had cracked in service were eliminated)
(b) a very large flaw tolerance
(c) a risk argument that was based on the finding that elimination of the inspection resulted in negligible change in core damage frequency

These arguments were accepted by the ASME Code, as well as the NRC, and Code Case N-648-1 was approved by ASME in December of 2000 [41].

The NRC, in a conditional acceptance of this Code Case, stated the following [42]: “In place of a UT examination, licensees may perform a visual examination with enhanced magnification that has a resolution sensitivity to detect a 1-mil width wire or crack,

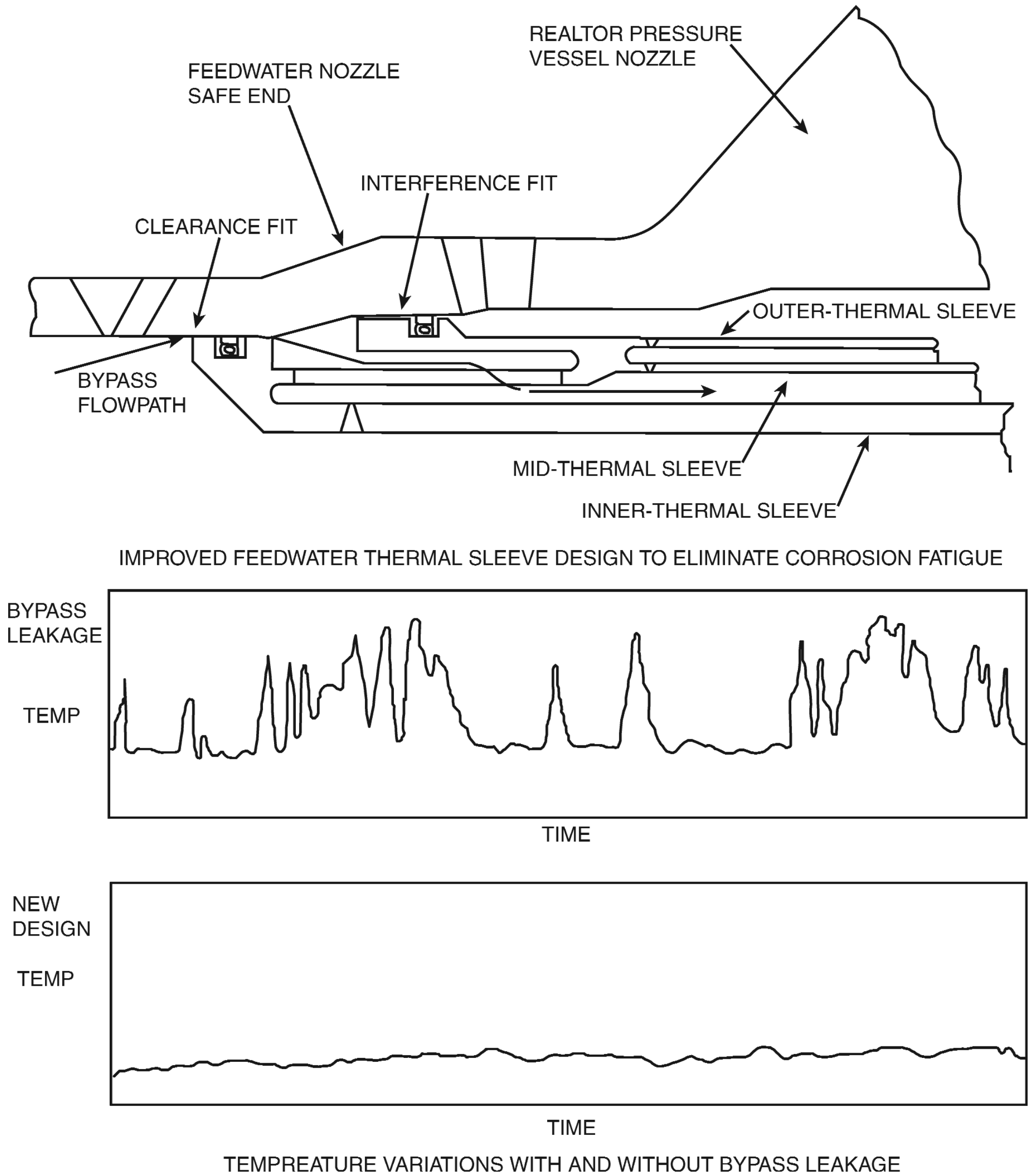

AQ: Please provide Fig.41.10 Callout.

FIG. 41.10 IMPROVED THERMAL SLEEVE DESIGN AND TEMPERATURE VARIATIONS WITH AND WITHOUT BYPASS

utilizing the allowable flaw length criteria of Table IWB-3512-1 with limiting assumptions on the flaw aspect ratio. The provisions of Table IWB-2500-1, Examination Category B-D, continue to apply except that, in place of examination volumes, the surfaces to be examined are the external surfaces shown in the figures applicable to this table." Thus, the NRC requires a more sensitive visual examination technique than that specified in the Code Case.

41.3.3.2 Alternate Inspection Frequency. Currently, BWR RPV nozzle inner radius and nozzle-to-shell welds are inspected per ASME BPVC Section XI requirements (Table IWB-3500-1, Examination Category B-D), which requires 100% inspection for each 10-year interval. These examinations are costly and result in significant radiation exposure to examiners. Since 1990, the performance of NDE has improved substantially such that there is a high reliability of detecting flaws that can challenge the structural integrity of BWR nozzles and their associated welds. Code Case 702 [43], approved at the December 2003 meeting of the Section XI Main Committee, allows a reduction of the nozzle-to-shell welds and nozzle blend radii from 100% to 25% of the nozzles every 10 years, 25% inspection each 10-year interval.

BWRVIP-108 [44], which provided the technical basis for this Code Case, described the technical approach as follows: "The project team evaluated the available field inspection data and performance demonstration data for BWR nozzles. They selected representative nozzles for the evaluation, including core spray, main steam, and recirculation inlet and outlet nozzles. PFM and deterministic fracture mechanics (DFM) calculations were performed to assess the reliability of the nozzles after implementing the revised inspection approach. The PFM code, VIPER, developed by the BWRVIP with a successful first use in BWRVIP-05, employs

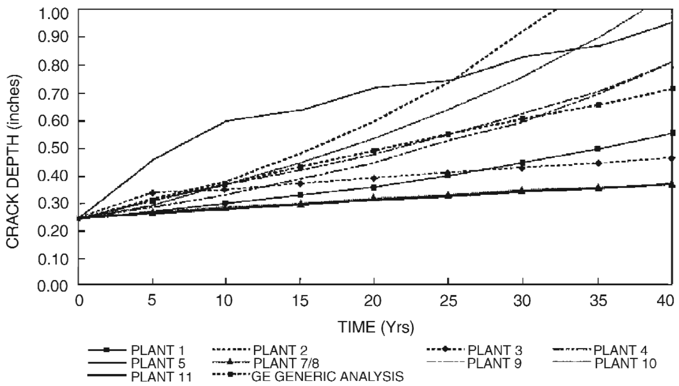

FIG. 41.11 FRACTURE MECHANICS RESULTS FOR SEVERAL BWRs

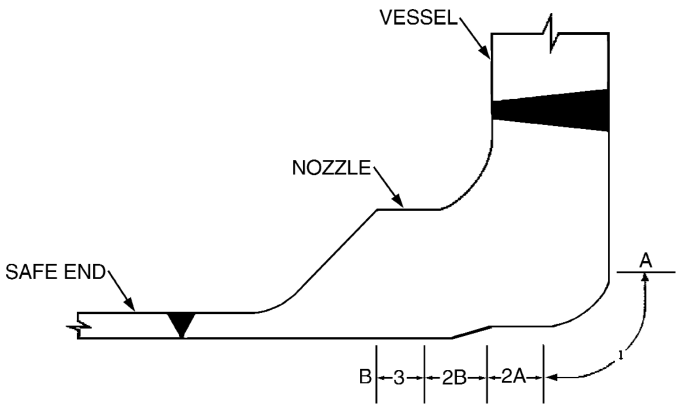

FIG. 41.12 BWR FEEDWATER NOZZLE INSPECTION ZONES (CLAD-REMOVED NOZZLE)

Monte Carlo methods to assess the reliability of a BWR RPV having flaw distributions, material properties, fluence distributions, and several other parameters, which are assumed to be randomly distributed. A DFM evaluation was also performed to demonstrate that expected flaws, based on field experience, would not jeopardize the structural integrity of the vessel. A flaw is selected that bounds any expected flaws based on field inspection results. Using appropriate material properties, a deterministic LEFM evaluation is performed to demonstrate that failure is not expected."

41.3.4 Stub Tube Cracking

The CRD and In-Core Housing penetrations in a BWR are on the bottom head of the vessel. The earlier BWR CRD penetrations used a stub tube to which the CRD housing is welded. The typical CRD housing is 6 in. in diameter and is made of either Type 304 stainless steel or Alloy 600. The use of the stub tube allows the stainless steel housing to be welded to the stub tube after post-weld heat treatment (PWHT) of the vessel. Figure 41.13 shows the typical CRD stub tube penetration in a BWR/2 bottom head. This is referred to as a set-in stub tube design since the stub tube is in a socket in the bottom head prior to welding. In some BWRs, the stub tube was made of Type 304 stainless steel and was welded to the bottom head before PWHT. The subsequent PWHT caused furnace sensitization of the stub tube making it susceptible to IGSCC with the exposure to a high-temperature, water environment. The cracking could occur in the HAZs of the welds and anywhere along the length of the sensitized stub tube.

Cracking and, in some case, leakage has been observed in BWR plants with furnace-sensitized stub tubes. The observed leakage has been well within the system leakage limits and has been a small fraction of the system makeup capability. Unlike the PWRs where the coolant uses borated water, there is no boron in the BWR water and leakage from the stub tube cracking does not lead to boron corrosion concerns. Stub tube cracking by itself does not pose a direct safety issue. Limiting the leakage has been the focus of the corrective action prior to plant startup. Roll expansion of the housing against the vessel penetration has been used to address the leakage concern. The plastic deformation of the housing against the vessel results in an effective leakage barrier.

The stub tube roll expansion repair has been used successfully in several BWRs and has been reviewed by the NRC staff. For the domestic BWR plants, the NRC typically approved the repair process as an alternative to the requirements of ASME BPVC Section XI, para. IWA-5250(a)(3) pursuant to 10 CFR 50.55a(a)(3)(I) on a case-by-case basis. Recently, the NRC allowed continued plant operation for the second cycle following discovery of CRD stub tube leakage in a BWR/2 plant [45]. Summary of the NRC's safety evaluation follows.

> The NRC staff concluded that, based on industry experience, roll expansion of the CRD housing to the RPV is an appropriate alternative repair for use at the BWR/2 plant. The roll expansion process will eliminate, or reduce to an acceptable

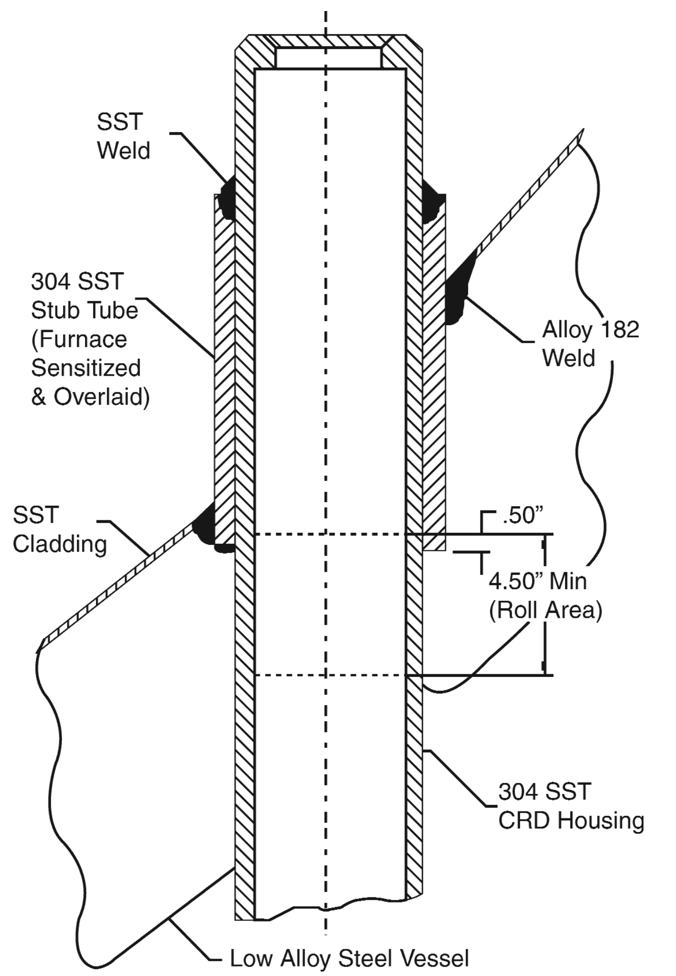

FIG. 41.13 A TYPICAL BWR SET-IN CRD STUB TUBE DESIGN

level, leakage from CRD housings. The housings will be plastically expanded within the RPV lower head bore to create a radial contact pressure between the housing and the vessel bore. Proper contact pressure is achieved by controlling the radial expansion of the housing and by utilizing additional passes to increase the contact length. The process will have no harmful effects on the CRD housing, stub tubes, or the reactor vessel. Potential failures, which could occur as a result of this repair, have been evaluated. The roll repair will meet the qualification criteria, without exception, and the nominal 3–5% minimum thinning to achieve continuous contact. Additionally, the alternative provides for the pre-repair and post-repair inspections to ensure the adequacy of this proposed repair. Thus, the proposed alternative will provide assurance of structural integrity for the approval period requested.

Imposition of the Code repair would require that the plant remain in a shutdown condition for an extended period in order to disassemble and remove fuel from the reactor to determine the exact leak location and to perform an in-vessel repair involving additional personnel exposure. Because use of the alternative repair (roll expansion) until the next refueling outage will provide adequate assurance of structural integrity, compliance with the specified requirements of the Code (a weld repair) would result in hardship or unusual difficulty without a compensating increase in the level of quality and safety.

The NRC staff has evaluated the licensee's proposed alternative for the plant. The staff finds that the proposed roll expansion repair, as described above, is acceptable until the next refueling outage. The NRC staff does not approve the roll-expansion process as a permanent repair in lieu of meeting the ASME Code repair criteria. The NRC staff recommends that if the licensee intends to use this alternative as a permanent repair, it should pursue this alternative repair of the CRD housings with the Code Committee to accept this as a permanent repair through a Code Case on an expedited basis. Should this prove to be not successful, the NRC staff recommends that the licensee follow up with a schedule for a permanent Code repair. The implementation of the alternative is subject to inspection by the NRC.

Based on the NRC's recommendation, the plant owner helped develop Code Case N-730 [46], the technical basis of which is documented in [47]. Reference 47 builds on the BWRVIP roll repair document [48] that was part of a full-scale effort to develop and qualify the roll repair process and equipment. A Code Case (tentatively assigned the number N-769) is currently under development for the roll repair of BWR bottom head in-core housing penetrations.

Other types of stub tube repair concepts include the following:

(a) a mechanical seal forming a pressure boundary around the weld
(b) a welded sleeve forming a pressure boundary and weld load path (see Fig. 41.14 for a typical example for a set-on stub tube [49])
(c) a replacement of the stub tube and housing

The replacement option involves welding close to the P3 vessel material where preheat or PWHT may not be feasible. Code Case N-606-1 [50] was specifically developed to permit the use of ambient temperature machine GTAW temper bead technique for BWR CRD housing/stub tube repairs.

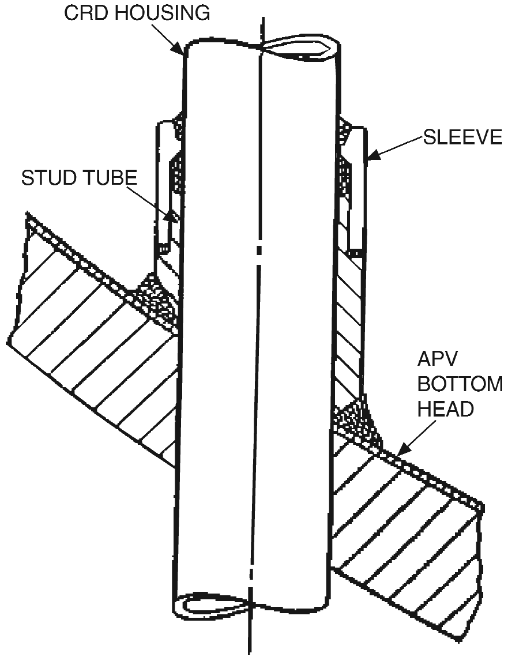

FIG. 41.14 STUB TUBE NARROW GROOVE WELDED PARTIAL DESIGN

41.3.5 Vessel Attachment Weld Cracking

There are numerous internal attachments to the BWR RPV that are welded using the alloy 182 that is known to be susceptible to SCC. Also, some attachments such as the jet pump riser brace are fatigue sensitive. One of the aspects that needs to be considered when field cracking is detected at an attachment weld is the potential for crack growth into the vessel material during future operation.

41.3.5.1 Vessel-to–Shroud Support Weld Cracking. In late 1999, stress corrosion cracks were discovered in alloy 182 welds in the shroud support structure of Tsuruga-1, a BWR-2 located in Japan (see Fig. 41.15). This weld material was used in the construction of the conical support structure as well as to attach the support structure to the RPV. These cracks were detected visually and confirmed with penetrant inspection as well as by metallography during core shroud replacement activities. The number of crack indications was more extensive than had been seen previously in BWRs and the cracks were located on the underside of the core support structure; thus, they could not be detected during routine visual inservice inspection from the top.

Following this finding, BWR owners were advised to review their inservice inspection programs and consider performing an examination of the RPV-to–shroud support plate weld [51]. Somewhat similar cracking on the underside of the H9 weld was detected at a U.S. BWR-2 plant though UT inspection conducted from outside the vessel. A fracture mechanics evaluation [52] was performed to address the following two issues:

(a) What is the structural margin during future operation at the shroud support in the presence of observed cracking?
(b) What is the number of years of plant operation until an assumed flaw at the clad base metal interface would be projected to grow into the base metal to allowable flaw depth calculated by the rules of ASME BPVC IWB-3600?

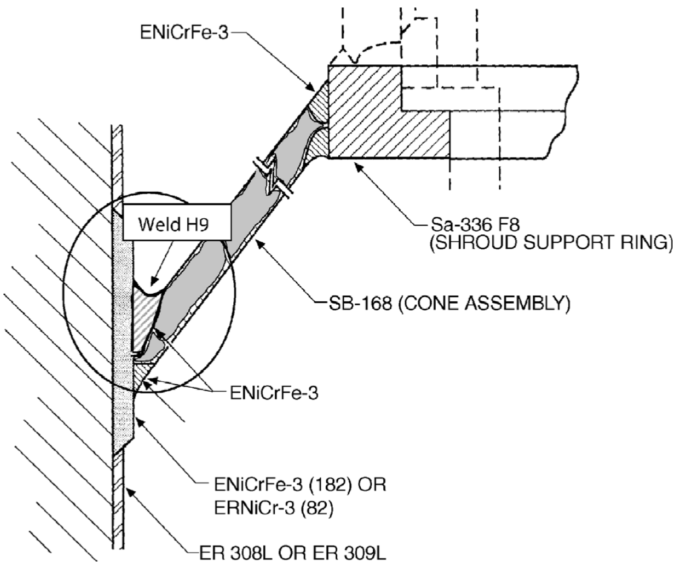

FIG. 41.15 BWR-2 SHROUD SUPPORT GEOMETRY

The evaluations conducted to address both of these issues considered projected crack growth from at least 80,000 hr (approximately 10 years) of future operation.

The detailed examinations during shroud replacement activities at the Japanese BWR-2 confirmed that none of the cracks entered the vessel low-alloy steel base metal adjacent to the weld metal. This clearly indicated that the cracking was confined to alloy 182 even though the plant had operated for over 25 years. Therefore, the fracture mechanics approach to quantify the allowable operating time conservatively considered a long axial flaw (aspect ratio of 0.1) placed at the depth of the clad low-alloy steel interface.

The stresses considered in the evaluation were those due to internal pressure, thermal expansion, cladding, and weld residual. The values of total applied stress intensity factor K as a function of crack depth a are shown in Fig. 41.16. The fatigue crack growth using the Appendix A curves was found to be insignificant. However, the potential crack growth due to stress corrosion cracking was taken into account using the following K versus da/dt relationship [53]:

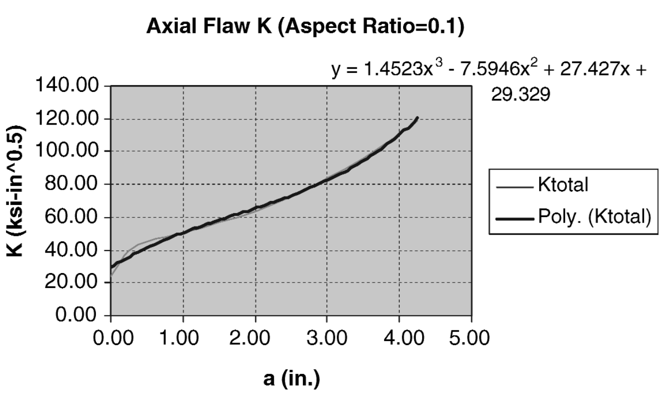

FIG. 41.16 CALCULATED VALUES OF TOTAL K AND THE POLYNOMIAL FIT

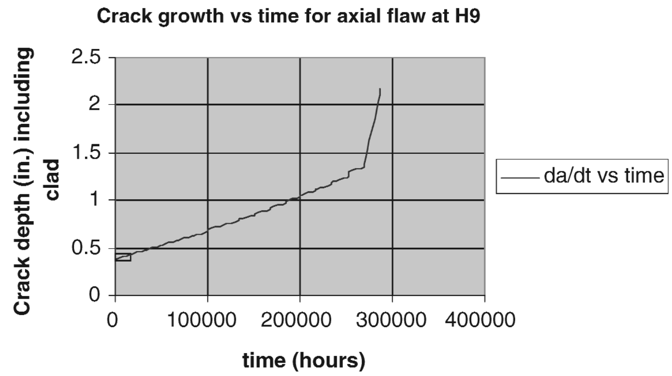

FIG. 41.17 PREDICTED CRACK GROWTH AS A FUNCTION OF OPERATING HOURS

$$da/dt = 2.8 \times 10^{-6} \quad \text{in./hr for } K < 50 \text{ ksi}\sqrt{\text{in.}} \tag{7}$$

$$6.82 \times 10^{-12}\,(K)^4 \quad \text{in./hr for transient condition, or } K < \text{ksi}\sqrt{\text{in.}} \tag{8}$$

For the purpose of the crack growth calculation, it was assumed that there would be approximately 800 hr of transient condition operation during a 2-year (approximately 16,000 hr) cycle of operation. The results of crack growth prediction are shown in Fig. 41.17. The allowable crack depth was determined to be 2 in. based on normal/upset conditions. Figure 41.17 indicates that this value of crack depth is reached in excess of 200,000 hours of operation. This flaw evaluation provided technical justification for continued operation of the RPV with the observed H9 weld cracks for at least 5 additional operating cycles, equivalent to 10 years of operation.

41.3.5.2 Steam-Dryer-Support-Bracket Cracking. Steam dryer support brackets are four stubby projections from the ID of the vessel that support the steam dryer. They are 3 × 5 × 11-in. tall forgings, full penetration welded to alloy 182 pads about 10 ft below the closure flange. Figure 41.18 shows the geometry of the cracked bracket [54]. A metallurgical analysis indicated that the bracket failed by a fatigue mechanism. During normal operation, the only design loads transferred between the steam dryer and the support brackets are vertical. The loads are transferred to the bracket through a seismic block, which provides horizontal restraint during earthquake loading. Examination of the failed bracket on the upper surface showed that the dryer support ring was in direct contact with the edge of the bracket farthest from the reactor wall due to an improperly positioned seismic block. This was different from the other three identical brackets that showed contact with the seismic block attached to the support ring. The point of application of the load on the failed bracket was 80% farther away from the crack initiation edge than was the load application point on the uncracked bracket 180° away from it. This meant 56% higher cyclic bending stresses at the failed bracket. Therefore, the corrective action for the cracked bracket was to replace it exactly as in the original design (same bracket material, configuration, and weld material) and to ensure that the seismic block was in contact with the bracket rather than the dryer support ring. A review of the ASME BPVC Section III fatigue design curve for Ni-Cr-Fe materials (ASME BPVC Section III, Fig. 19.2) indicated that a 56% improvement in stress would translate into a fatigue life improvement by a factor of at least 25. This meant that

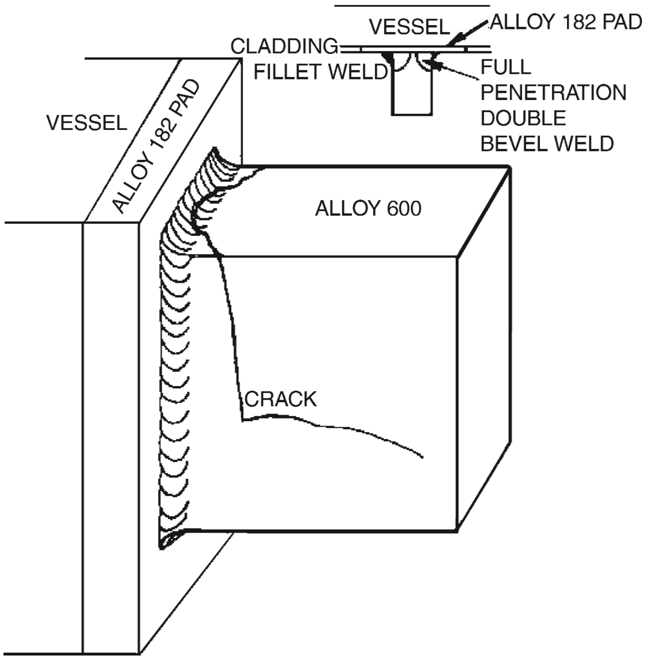

FIG. 41.18 STEAM DRYER SUPPORT BRACKET CRACK

the repair extended the life of the bracket significantly past the vessel design life. A VT examination after 1 year of service revealed that this bracket was free of cracks.

41.3.6 Low Upper Shelf Energy Evaluation

41.3.6.1 Background. Appendix G of 10 CFR50 [52] states that the RPV must maintain upper-shelf energy (USE) throughout its life of no less than 50 ft-lb, unless it is demonstrated, in a manner approved by the director of the office of Nuclear Reactor Regulation, that lower values of USE will provide margins of safety against fracture equivalent to those required by Appendix G of ASME BPVC Section XI. Regulatory Guide 1.99, Revision 2 [56] provides a method to estimate the decrease in USE as a function of fluence and copper content. It was recognized in the early 1980s that some RPVs have materials for which the USE may fall below 50 ft-lb due to irradiation embrittlement. In 1982, the NRC published proposed procedures for the analyses required by 10 CFR50 for operating RPVs as NUREG-0744 [57]. At the time of publication of this document, the NRC officially requested that the ASME Code recommend criteria, analysis methods, and suitable specifications for material properties to be used for the assessment of reactor vessels that do not meet the Charpy USE requirements. As a result of this request, the Section XI Working Group (WG) on Flaw Evaluation developed, through an approximately 10-year effort, acceptance criteria and acceptable analysis methods to address this issue. The WG also developed simplified evaluation procedures applicable for use in evaluations of Service Level A and B conditions. WRC Bulletin 413 [58] documents the results of the WG's effort; Part 1 of the Bulletin contains the basis for the recommendations sent from the WG to the NRC, dated January 11, 1991. These recommendations included the acceptance criteria that were subsequently implemented as Code Case N-512 [59] and later as Nonmandatory Appendix K in ASME BPVC Section XI. Part 2 of the Bulletin contains the basis for the simplified evaluation procedures for Service Level A and B conditions. The NRC published Regulatory Guide 1.161 [60] to provide additional guidance to include analysis procedures for Service Levels C and D, guidance on selecting the transients for evaluation, and details on temperature-dependent material properties. The low USE analysis also has been called equivalent margin analysis.

For the evaluation of Level A and B service conditions, a $\frac{1}{4}t$ surface flaw with an aspect ratio of 6:1 oriented axially or circumferentially (whichever direction is relevant) is postulated. The two criteria to be satisfied are the following.

(a) The applied J-integral, evaluated at a pressure that is 1.15 times the accumulation pressure as defined in the plant-specific Overpressure Protection Report, with a factor of safety of 1.0 on thermal loading for the plant-specified heat-up/cool-down conditions, shall be shown to be less than $J_{0.1}$, the J-integral characteristic of the material resistance to ductile tearing at a flaw growth of 0.1 in.
(b) The flaw shall be shown to be stable, with the possibility of ductile flaw growth at a pressure that is 1.25 times the accumulation pressure defined in (*a*), with a safety factor of 1.0 on thermal loading.

The J-R curve shall be a conservative representation for the vessel material under evaluation. The criteria for the evaluation of Level C service conditions are essentially the same, except that the postulated flaw is $\frac{1}{10}t$ deep and the safety factor on the pressure loading is 1.0. Additional relaxation in the criteria for Level D service conditions is that a best estimate J-R curve can be used.

41.3.6.2 Generic BWR Evaluation. In September 1992, the NRC, in discussing the preliminary review of the responses to Generic Letter 92-01, strongly recommended that equivalent margin analyses be done by the Owners Group. The BWR Owners Group developed a generic analysis in the form of a topical report [61]. The objective was to provide a safety net analysis for plants that could not quantitatively demonstrate, using NRC-approved methods, that USE would remain above 50 ft-lb and might, therefore, be subject to regulatory action. A second objective, which developed within the BWR Owners Group in the process of performing the analysis, was to provide a topical report, which could be referenced by utilities as part of their licensing basis, to address compliance with the 50 ft-lb requirement on USE in 10 CFR50 Appendix G.

Both the axial and circumferential flaws in plate material, with the corresponding longitudinal and transverse USE data, were considered in the analysis. For welds, only the more limiting axial flaw case was evaluated. The analysis addressed BWR/2 plates separately from BWR/3–6 plates, due to differences in geometries, material properties, and availability of USE data. The welds were addressed together for BWR/2–6 vessels but were grouped by weld type, specifically shielded metal arc, electroslag, and submerged arc welding.

Figure 41.19 shows the Level C condition transient used in the analysis, and Figure 41.20 shows the results for $J_{0.1}$ assessment also for Level C conditions. Topical report was reviewed and approved by the NRC [62]. Table 41.3 (Table 1 [62]) provides a summary of the results. Equivalent margin was demonstrated for 35 ft-lb USE values, except in the longitudinal plate direction where the results were 50 ft-lb for BWR/2 plates and 59 ft-lb for BWR/3 – 6 plates. The analysis results for Levels C

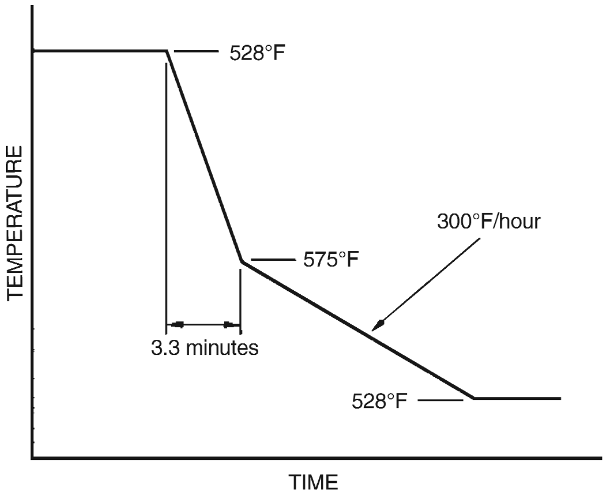

FIG. 41.19 TEMPERATURE-TIME VARIATIONS DURING AUTOMATIC BLOWDOWN TRANSIENT (LEVEL C CONDITION)

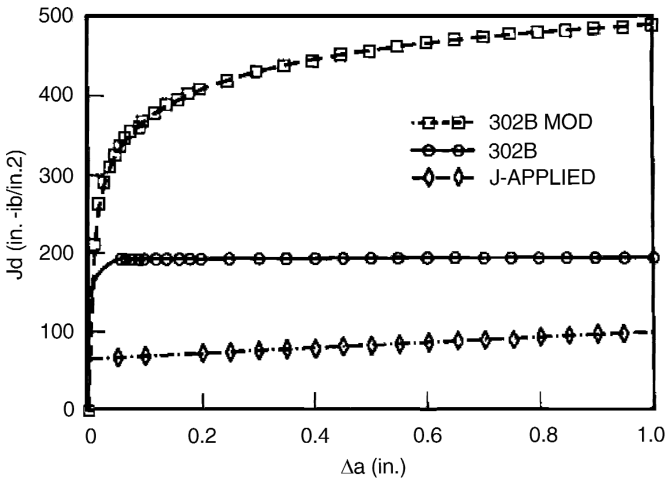

FIG. 41.20 $J_{0.1}$ ASSESSMENT FOR LEVEL C CONDITIONS

and D conditions were less limiting than Levels A and B conditions. The material property projections used 32 effective full-power years (EFPY), which is taken to be the equivalent to 40 years of operation. Table 41.3 also shows the NRC-predicted end-of-life USE values.

Specific BWR plants can compare their USE surveillance results to the predictions of Regulatory Guide 1.99 to verify that the comparisons of 32 EFPY USE with the equivalent margin analysis are bounding for their vessel beltline, using a worksheet [61]. Once the bounding nature of the BWR Owners Group analysis has been established, the plant can reference the analysis [61] to demonstrate compliance with the USE requirements of 10 CFR50 Appendix G for 32 EFPY of operation.

41.4 REACTOR PRESSURE BOUNDARY PIPING

The BWR reactor pressure boundary piping material is typically either carbon steel (SA-106, Grade B, SA-333, Grade 6, and SA-516 Grade 70) or stainless steel (Type 304 or 316, regular carbon, L grade, or LN grade). The safe end material could also be Ni-Cr-Fe material (SB-166). The experience with the BWR carbon steel piping has been excellent and there is no field degradation incidents attributed to it. On the other hand, the BWR stainless steel piping (made of Type 304/316) has experienced cracking during service [63–65]. As discussed later, the development of Appendix C of ASME BPVC Section XI in the early 1980s and several Code Cases were intended to provide guidance in the evaluation and repair of this type of stainless steel pipe cracking.

41.4.1 Cause of Cracking

Cracking in weld-sensitized Type 304 stainless steel piping has been mainly due to IGSCC. The IGSCC mechanism requires a combination of sensitized material condition, high-sustained stress, and susceptible environment. Weld sensitization results in carbide precipitation in the HAZ leaving a region of IGSCC susceptible material. Applied stress coupled with weld residual stresses provide conditions that could cause cracking. Finally, the

TABLE 41.3 BWR RPV EQUIVALENT MARGIN REVIEW SUMMARY [57]

Summary on results from equivalent margin analysis for eight types of beltline material

MATERIAL TYPE	CU %	FLUENCE $\times 10^{18}$ (n/cm^2)	INI. USE (ft-lb)	PREDICTED USE DROP %	PREDICTED EOL USE BWROG (ft-lb)	PREDICTED EOL USE NRC (FT-LB)	CODE CASE N-512 EOL USE (ft-lb)	NUREG/ CR-6023 EOL USE (FT-LB)
BWR/2 (L)*	.27	2.4	76	26	56	—	50 [45]**	55
BWR/2 (T)	.27	2.4	49	26	36.5	—	35 [25]	36
BWR/3-6 (L)***	.17	3.8	91	21	72	78	59 [59]	55
BWR/3-6 (T)	.17	3.8	59	21	47	51	35 [25]	36
SMAW	.35	2.4	87	34	57	56	35 [33]	33
ELECTROSLAG	.35	2.4	69	34	46	36	35 [33]	33
NON-LINDE 80	.35	2.4	71	34	47	46	35 [33]	33
LINDE 80	.31	1.0	—	—	—	—		33

* Containing SA302B plates only.

** Values inside brackets are estimated by the staff directly from Figures 5-2a, b, 5-3a, b, and 5-4 of the topical report, which represent the lowest limits that the USE values of beltline materials may reach. These values are only used to assess margins; they do not represent the minimum permissible USE values acceptable to the staff.

*** Containing SA302B Modified and 533B plates.

high-temperature oxygenated water provides the environmental conditions needed for IGSCC. The IGSCC is explained by the presence of the three necessary conditions for cracking.

41.4.2 Remedial/Mitigation/Repair Measures

In October 1979, in response to the increased number of incidents of IGSCC of austenitic stainless steel piping in BWRs and the appearance of cracking in large-diameter (24–28 in.) recirculation system piping, a group of BWR utilities organized an Owners Group to provide the R&D resources necessary to solve the pipe-cracking problem. EPRI was given the responsibility of integrating these resources into ongoing research and development efforts funded by EPRI, the BWR Owners, and GE so as to establish a single, unified industry program addressing pipe cracking in BWRs. Most overseas BWR Owners also participated in the resulting program, known as the BWR Owners Group IGSCC Research Program, which began in 1979 and was completed in 1988 [66–68].

The initial set of IGSCC remedies was referred to as near term. These remedies could be applied to susceptible Type 304 stainless steel components in the short term to field repairs and replacements and to plants under construction that were committed to the use of Type 304 stainless steel piping. The near-term remedies included solution heat treatment (SHT), corrosion-resistant cladding (CRC), and heat-sink welding (HSW). Following welding, SHT redissolves grain-boundary carbides and restores the grain-boundary chromium concentration. CRC consists of cladding the susceptible part of the pipe inside the surface adjacent to the girth weld with SCC-resistant duplex weld metal. HSW is designed to generate compressive residual stresses at the ID of the HAZ through the use of carefully controlled welding parameters in conjunction with water cooling of the inside of the pipe during welding.

To mitigate IGSCC in operating piping, induction heating stress improvement (IHSI) and last-pass heat sink welding (LPHSW) were also qualified in the early 1980s. IHSI modifies the as-welded residual stresses by inducing small amounts of plastic deformation in the HAZ. This is accomplished by generating a through-wall temperature gradient (by induction heating the outside of the pipe and water cooling the inside) that is sufficient to cause a small amount of yielding. The LPHSW is essentially similar to HSW except that it only involves remelting the weld crown while providing a heat sink and, therefore, can be applied to existing welds. Mechanical stress improvement (MSIP) has also been used to favorably modify the weld residual stresses in HAZ [69]. In MSIP, a similar result as IHSI is obtained by hydraulically squeezing the pipe adjacent to the HAZ to induce a small amount of plasticity.

IGSCC-resistant piping materials (Type 316 nuclear grade and Type 304 nuclear grade stainless steel) were also developed as the materials remedy for replacement piping. All stress- and sensitization-related remedies are limited to the specific component to which they are applied. In contrast, environment-related remedies have the potential of protecting the whole coolant system. Laboratory and field studies demonstrated that electrochemical corrosion potential (ECP) of stainless steel in the recirculation systems of operating BWRs can be reduced to low values by injecting hydrogen into the feedwater (hence the name hydrogen water chemistry) and that IGSCC is suppressed when the ECP is below −230 mV SHE.

Stress improvement remedies and hydrogen water chemistry were effective in retarding the further growth of shallow cracks; however, sometimes deep cracks were observed, particularly in the alloy 182 butter at the low-alloy steel nozzles. The dissimilar metal weldment joining the BWR nozzles to safe ends is one of the more complex configurations in the entire recirculation system. Field installation techniques typically specify that a special shop weld deposit (butter) be placed on the end of the nozzle prior to final shop PWHT to facilitate field welding without PWHT. Many BWR vessels used Inconel 182 manual shielded metal arc electrodes to weld deposit the butter. Later laboratory studies determined that alloy 182 was susceptible to IGSCC, especially under severe conditions such as crevices and/or cold work. Repair/replacement activities at two BWRs, where axially oriented IGSCC from the butter progressed into the low-alloy steel nozzle, have been described [70]. Many BWR plant owners proactively undertook repair/replacement/mitigation activities to address potential IGSCC of alloy 182 butters [71].

Weld overlay type of repair is also a very attractive remedy and has been used extensively in the field. It is applicable both at the pipe-to-pipe welds and at pipe-to-nozzle or safe-end welds.

41.4.3 Weld Overlay Repairs

Weld overlays were first applied in 1982 as a repair for IGSCC in stainless steel piping [72]. As shown in Fig. 41.21, the repair technique is based on the application of weld metal to the outside pipe surface over and to either side of the flawed location, extending circumferentially 360°. The weld overlay repair performs the following functions:

(a) It provides structural reinforcement of the flawed location, such that adequate load-carrying capability is provided, either in the overlay by itself or in some combination of the overlay and the original pipe wall thickness.
(b) It provides a barrier of IGSCC-resistant material to prevent IGSCC propagation into the overlay weld metal.
(c) It introduces a compressive residual stress distribution in at least the inner portion of the pipe wall, which will inhibit IGSCC initiation and propagation in the original pipe joint.
(d) It prevents local leakage from small axial flaws.

Although these repairs were accepted by the NRC, the early regulatory position was that such repairs were only interim measures. The utilities were allowed to operate for two fuel cycles with weld overlay repairs to enable them to develop and adequately plan for replacement activities. In NUREG-0313, Revision 2 [9], the NRC

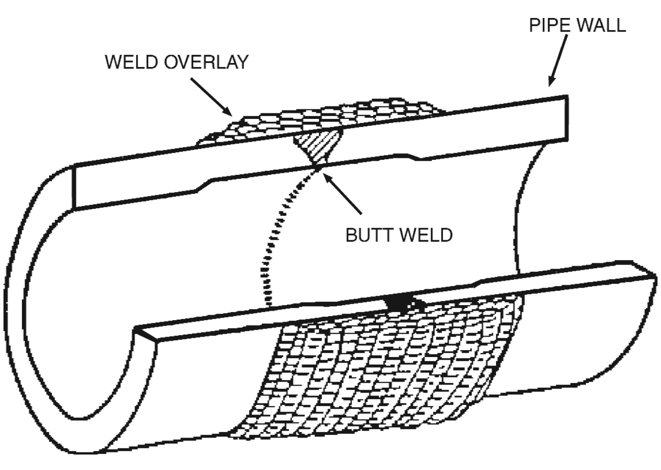

FIG. 41.21 WELD OVERLAY REPAIR

indicated that, "If it is desired to operate for more than two fuel cycles with overlay reinforcement repair, the overlayed weldments should be inspected to ensure that the overlays will continue to provide the necessary safety margin." The BWR Owners Group and EPRI in the meanwhile conducted several inspections, weld residual stress measurement, and fracture toughness studies on weld overlays [73–75] to justify their long-term operation. In 1992, the ASME BPVC Code published Code Case 504 [76] specifically addressing the weld-overlay-type repair of cracked austenitic stainless steel piping.

41.4.3.1 Code Case 504. The Code Case specifies various requirements for implementing weld overlay repairs, such as weld metal composition, surface preparation, design, pressure testing, and examination. Some of these requirements are discussed.

The requirement (e) specifies that the first layer of weld metal with delta ferrite content of at least 7.5 FN shall constitute the first layer of the weld reinforcement design thickness. Generally, ferrite readings are taken at the weld center and edge of the weld crown in the overlay layer at each of the quadrants. The values are averaged for comparison with the minimum required value. Lower values, but no less than 5 FN, may be acceptable based on evaluation.

The design considered in (f)(1) is what is called as the full structural or standard weld overlay. The flaw is assumed to be 100% through the original pipe wall thickness for the entire circumference of the pipe. The advantage of this design is that any uncertainty in the sizing of the original crack(s) is unimportant for this case. The thickness of the full structural weld overlay can be based on either the Tables given in ASME BPVC IWB-3640 or the source equations in Appendix C of ASME BPVC Section XI. The source equations in Appendix C [77,78] typically provide smaller thickness. The reason is that the membrane stress (P_m) used in the source equations is the calculated value and is typically smaller than the assumed P_m of 0.5 S_m in the Tables. The source equations applicable to full structural weld overlay are the following:

$$\beta = \pi(1 - a/t - P_m/\sigma_f)/(2 - a/t) \tag{9}$$

$$P_{bc} = (2\sigma_f/\pi)(2 - a/t)\sin(\beta) \tag{10}$$

$$P_{bc} + P_m = \mathrm{SF}\,(P_m + P_b) \tag{11}$$

where

σ_f = material flow stress = $3S_m$
S_m = material design stress intensity
P_m = primary membrane stress
P_b = primary bending stress
P_{bc} = failure bending stress
a = crack depth (equal to pipe thickness)
t = total thickness (pipe wall + weld overlay thickness)
SF = safety factor
= 2.77 for normal/upset conditions
= 1.39 for emergency/faulted conditions

The weld overlays are typically applied using gas tungsten arc welding (GTAW), a nonflux welding process. Therefore, only the primary stresses are used in the above equations. The primary loading is typically the internal pressure, weight, and seismic inertia. The membrane and bending stresses are calculated on the basis of overall thickness including the weld overlay thickness. Therefore, an iterative solution of Eqs. (9) through (11) is necessary to calculate the required weld overlay thickness. The ASME BPVC IWB-3640 rules require the a/t value to be ≤ 0.75. In many cases, this criterion would require an increase in the calculated thickness. Although not explicitly stated in the rules of ASME BPVC IWB-3640, the weld overlay design thickness is also typically evaluated against the primary stress limits of the Code of Construction. For Class 1 components such as piping, ASME BPVC IWB-3610(d)(2) states that a component containing the flaw is acceptable for continued service during the evaluated time period if the primary stress limits of ASME BPVC NB-3000, assuming a local area reduction of the pressure-retaining membrane that is equal to the area of the detected flaw.

The Code Case also provides guidance for overlay thickness determination when fewer than five axial flaws and/or short circumferential flaws (less than 10% of circumference) are present at a weld. The specified overlay length is at least 0.75 $\sqrt{(Rt)}$ beyond each end of the observed flaws, where R and t are the outer radius and nominal wall thickness of the pipe prior to depositing the weld overlay. The circumferential cracks are generally assumed to be located axially at the end of the HAZ. If the cracked weld has on one side a larger thickness component such as a valve, the overlay can be terminated in the length direction where the valve section thickness is equal to the pipe thickness plus overlay thickness.

The results of experiments conducted to assess the adequacy of the thickness design equations for the weld overlay repairs (WORs) are documented [79]. The maximum stress from each of the four WOR pipe experiments conducted was significantly higher than that predicted by the ASME BPVC IWB-3640 analysis for a full structural overlay. The calculated safety factors were 30% higher than those used in the Code. The margins were slightly lower when actual flaw dimensions were used.

Application of weld overlays typically is performed with water backing on the inside of the weld to be repaired, which produces a through-wall gradient. The temperature difference, coupled with the normally occurring shrinkage of the overlay weld metal, has been shown to produce a highly favorable residual stress distribution in the pipe wall [80]. A favorable stress distribution is the one when combined with the applied stress distribution produces a nonpositive calculated value of stress intensity factor at a crack depth equal to the pipe thickness. This ensures nonpropagation of the IGSCC cracking during future operation. In some cases, the structural configuration may be such that water backing is not feasible; then, typically an application-specific finite element residual stress analysis is conducted to demonstrate that a favorable residual stress distribution is produced following the weld overlay.

Weld overlay application results in both radial and axial shrinkage at the repaired weld. Axial shrinkage magnitude is a function of the pipe diameter, weld overlay length, and the number of weld layers applied. Field measurements suggest that the bulk of the shrinkage occurs as a result of application of the first two layers. Generally, a finite element model of the piping system is required to calculate the shrinkage stresses at the various locations in the system. These shrinkage stresses are steady state secondary stresses of the cold-spring type and are not explicitly factored into the equations of ASME BPVC Section III, NB-3650; NB-3672.8 limits the cold springing stress to $2S_m$. However, the shrinkage stresses due to weld overlay are typically limited to a smaller value equal to the yield strength at temperature. In the evaluation of other flawed locations in the piping system, the calculated axial shrinkage stress shall be included as an expansion stress (P_e).

The axial shrinkage may result in changed air gaps of pipe whip restraints, the normal set points of variable spring hangers, and so on. Therefore, the Code Case requires the evaluation of system restraints, supports, and snubbers to determine whether design tolerances are exceeded. The non-mandatory Appendix O [81] of ASME Section XI also provides additional design, examination and inspection guidance for austenitic stainless steel weld overlay repairs.

41.4.3.2 Dissimilar Metal Weld Overlays. With the development of the weld overlay repair as an acceptable long-term repair measure to primary system austenitic stainless steel pressure boundary piping, industry attention had expanded to those pressure boundary joints that do not fall within this family of acceptable joints for weld overlay repair. In a BWR recirculation system, the inlet and outlet nozzle joints, where the low-alloy steel nozzle is welded to an austenitic safe-end material, represent a special weld overlay repair case not covered by Code Case 504. IGSCC had been observed in the Inconel 182 butter to the low-alloy steel nozzles. As a result, an Inconel 82 weld overlay repair technique was developed for application to a low-alloy steel nozzle to stainless steel or Inconel 600 safe end [82]. The alloy 82 weld overlay repair could also be used at a weld joint between an austenitic stainless steel pipe and alloy 600 safe end.

The repair approach consisted of a full structural weld overlay, using automatic GTAW technique deposited in accordance with a temper-bead-welding approach similar to that presented in Code Case N-432 [83]. The temper bead technique generally requires the application of elevated preheat, specific bead/layer formation, heat input controls, and a postweld heat treatment (PWHT). The preheat and PWHT requirements are specified primarily to preclude the introduction of hydrogen into the final weld. Hydrogen, the source of delayed cracking in the base material HAZ, is of primary concern when welding ferritic materials. Preheat is intended to eliminate moisture and contaminants that could be introduced into the molten metal during welding. PWHT allows the hydrogen potentially trapped in the HAZ and weld metal to diffuse out.

A later Code Case, N-638 [84], allowed an ambient temperature temper bead welding without the use of preheat or PWHT for implementation. This technique is applicable to both the similar (e.g., austenitic pipe to pipe) and dissimilar (e.g., safe end to nozzle) metal weld overlay repairs.

Figure 41.22 shows an example of the dissimilar metal weld overlay. Code Case 504 currently does not cover dissimilar weld overlays; therefore, this Code Case was used only as a guide in the design of this weld overlay. The provision regarding ferrite number does not apply to alloy 82 weld overlays. The weld overlay thickness was determined using the source equations in ASME BPVC Appendix C using S_m value for alloy 600 materials. Note that the length of the weld overlay in Fig. 41.22 is slightly larger (by the shaded length) to facilitate its inspection. Except for the flat surface requirement for UT inspection, the minimum thickness requirement is optional in the shaded area. At the safe end side, the weld overlay was terminated where the pipe plus overlay thickness exceeds the safe-end thickness. Alloy 82 weld metal has been used in some early dissimilar metal weld overlay repairs; nevertheless, more recently, Alloy 52 has been used in most applications.

The ASME Code has now developed the Code Case N-740 [85] to cover the application of dissimilar metal weld overlay repairs.

41.4.3.3 Impact of Revised ASME BPVC Section XI, Appendix C (2002 Addenda). Prior to the 2002 Addenda of ASME BPVC Section XI, the safety factors for the evaluation of

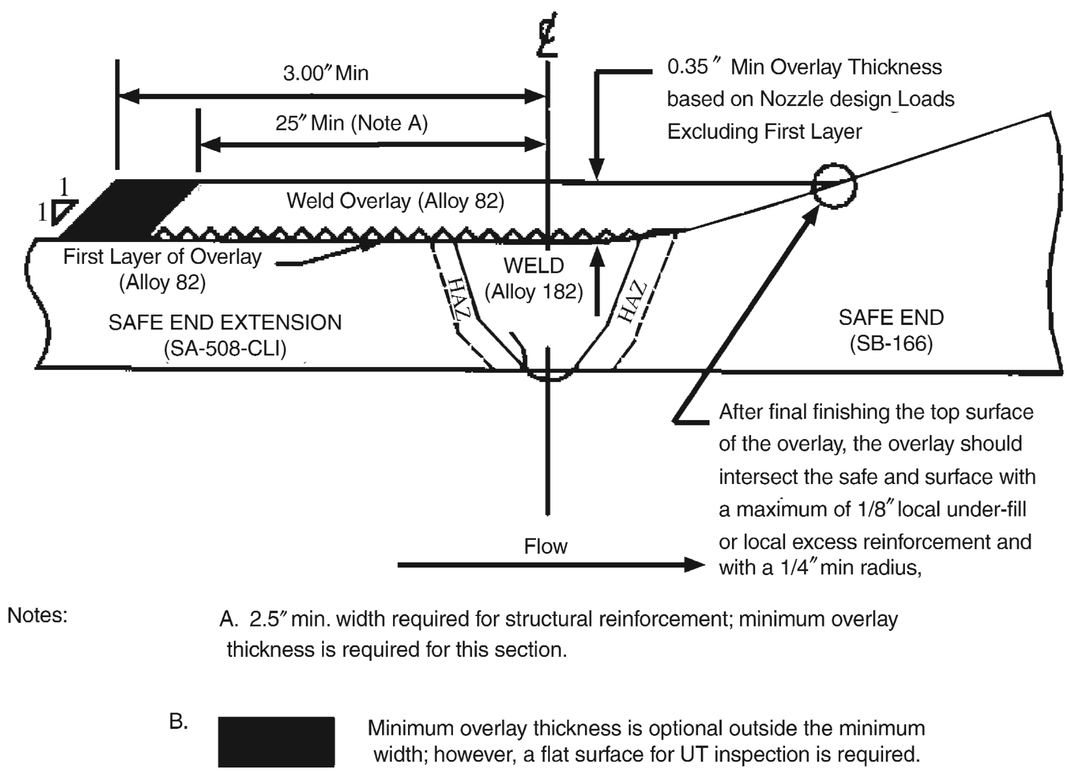

FIG. 41.22 CORE SPRAY SAFE END TO SAFE-END EXTENSION WELD OVERLAY

flawed austenitic piping, specified in Appendix C and referenced in ASME BPVC IWB-3640, were 2.77 for normal and upset conditions and 1.39 for emergency and faulted conditions [see Eq. (11)]. These safety factors were revised when a revised Appendix C was included in the 2002 Addenda [86]. Example calculations to assess the impact of the revised safety factors on existing evaluations of weld overlay repairs were performed [87,88]. The pipe material was Type 304 austenitic stainless steel, and the service temperature was assumed as 550°F. A summary of the calculations of the required weld overlay thickness values for three welds is given in Table 41.4. Required weld overlay thickness values from acceptance criteria on ($\sigma_m + \sigma_b$) in the 2001 Edition of Section XI were governed by Service Level B (upset condition). Required weld overlay thickness values from acceptance criterion on ($\sigma_m + \sigma_b$) in the 2002 Addenda to Section XI were governed either by Service Level B or C (emergency) condition, while required weld overlay thickness values from the separate acceptance criterion on 6_m in the 2002 Addenda were governed by Service Level B. The required weld overlay thickness values from the governing criterion for each weld are highlighted in bold italic in Table 41.4, and these are governed by the ASME BPVC Section III, NB-3200, primary stress intensity limits. Based on these results, it was concluded that there is no significant impact of the revised safety factors in the 2002 Addenda to Section XI on the required thickness of the weld overlay repairs.

The revised safety factors in Section XI, Appendix C, of the 2002 Addenda are also applicable Ni-Cr-Fe materials (Alloy 600 base metal and Alloy 82 or 52 welding materials) .

41.5 CRACK INITIATION, GROWTH RELATIONSHIPS, AND PLANT MONITORING

Protection against fatigue crack initiation through an explicit calculation of cumulative fatigue usage factor, is one of the design criteria for ASME Code Sections III and VIII (Division 2) pressure-retaining components. Protection against SCC type of crack initiation is not currently covered in the Code. However, several mitigation measures have been used by the BWR plant owners as indicated by the discussion in earlier paragraphs (e.g., para. 4.2 for BWR NSSS piping). When a component is inspected and found to have cracking, the appropriate crack growth rate relationship is an essential element in the flaw evaluation to justify continued operation. The cyclic loading aspects are covered in Chapter 39. Some of the unique aspects of fatigue evaluations for BWRs and the SCC growth rate relationships are discussed. A comprehensive review of the fatigue and SCC crack growth rate relationships in BWR water environment in provided in Reference 89.

41.5.1 Fatigue Initiation

The scope and intent of the ASME BPVC Section III fatigue design procedure was articulated in a presentation by Dr. William Cooper to the PVRC Workshop on the Environmental Effects on Fatigue Performance in January 1992 [90]. Some of the points of this presentation are summarized.

(a) The Design-by-Analysis procedure included several related considerations; however, the purpose for adding fatigue as one of the failure modes was to ensure that the reduction of the nominal safety factor from four to three did not result in a decrease in reliability if the vessel was expected to be subjected to cyclic operating conditions. The fatigue design procedures were intended to provide confidence that the component could be placed in service safely, not necessarily to provide a valid measure of actual component service life.

(b) The cyclic loading conditions defined in the Owner's Design Specification were not intended to represent a commitment on how the vessel was to be operated, only that the design transient definitions should provide useful information. For example, if an Owner were able to show the Design Specification included a cyclic event more severe than an event actually experienced, this would verify that the vessel was not subjected to an unevaluated condition.

41.5.1.1 Actual Versus Design Cyclic Duty. As pointed out in the preceding, the number and severity of cyclic events may differ from those specified in the design specification. Figure 41.23 shows a comparison of the actual number of transient events compared to the design basis for a typical BWR plant [91]. It is seen that the actual number of transients (such as startup and shutdown or SCRAM events) experienced at some operating reactors may be higher than that expected in the design basis. However, the severity

TABLE 41.4 COMPARISON OF REQUIRED THICKNESS OF WELD OVERLAY REPAIR

WELD	PIPE D, in. (mm)	PIPE NOMINAL t, in. (mm)	PIPE NOMINAL σ_m FOR ASME LEVELS B AND C, ksi (MPa)	PIPE NOMINAL σ_m ksi (Mpa)		REQUIRED WELD OVERLAY THICKNESS (in. (mm)) BASED ON:					
				ASME LEVEL B	ASME LEVEL C	2001 EDITION SECT. XI CRITERIA	2002 ADDENDA SECT. XI CRITERIA FOR $\sigma_m + \sigma_b$	2002 ADDENDA SECT. XI CRITERIA FOR σ_m	SECT. XI 0.75t CRITERION	SECT. III LIMIT ON P_m	SECT. III LIMIT ON $P_m + P_b$
DSRHR-3-II	20.0 (508)	1.25 (32)	5.5 (38)	5.2 (36)	10.2 (70)	0.43 (11)	0.48 (12)	0.40 (10)	0.42 (11)	0.41 (10)	***0.52 (13)***
24A-R-13	20.0 (508)	1.15 (29)	7.75 (53)	5.39 (37)	9.75 (67)	0.49 (12)	0.52 (13)	0.52 (13)	0.38 (10)	0.53 (14)	***0.59 (15)***
12BR-A-4	12.75 (324)	0.75 (19)	6.67 (46)	3.13 (22)	4.83 (33)	0.25 (6)	0.25 (6)	0.29 (7)	0.25 (6)	***0.30 (8)***	***0.29 (7)***

Notes:
(1) Required weld overlay thickness from the governing criterion is in bold italics.

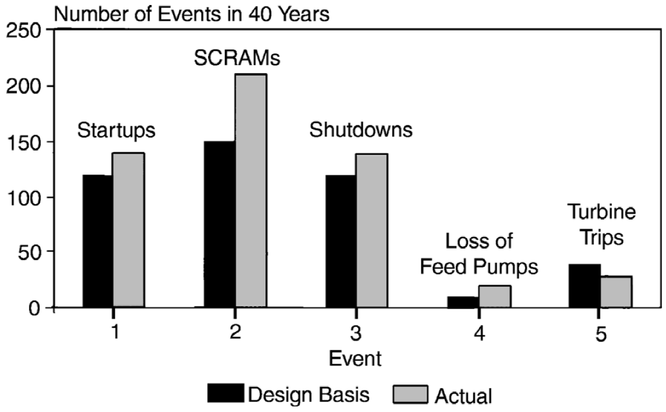

FIG. 41.23 DESIGN VERSUS ACTUAL NUMBER OF TRANSIENT EVENTS FOR A TYPICAL BWR PLANT

of the actual transient events (i.e., temperature and pressure fluctuations) is typically significantly lower than that assumed in the design basis. Figure 41.24 shows a comparison of the assumed design basis event and the actual transient based on measured temperatures; the number of actual transients may be higher but they are often less severe than the design basis, and the overall fatigue usage may be lower. In this respect, online, continuous monitoring of system transients and keeping track of the resulting fatigue usage in critical plant components offer important benefits in meeting plant licensing basis. The technical basis and the results of online fatigue usage monitoring at some BWR plants has been described [92,93]. In most cases, the calculated fatigue usage by the fatigue monitor was an order of magnitude lower than that calculated by design basis transient.

ASME BPVC Section XI, IWB-3740 and Nonmandatory Appendix L permit the fatigue usage factor reevaluation for a component in service. If the recalculated fatigue usage is greater than 1.0, flaw tolerance evaluation procedures can be used to demonstrate acceptance of a component for service.

41.5.1.2 Environmental Fatigue Effects. The current Section III fatigue design curves were based primarily on strain-controlled fatigue tests of small polished specimen at room temperature in air. Higuchi and Iida [94] demonstrated that the fatigue life of carbon

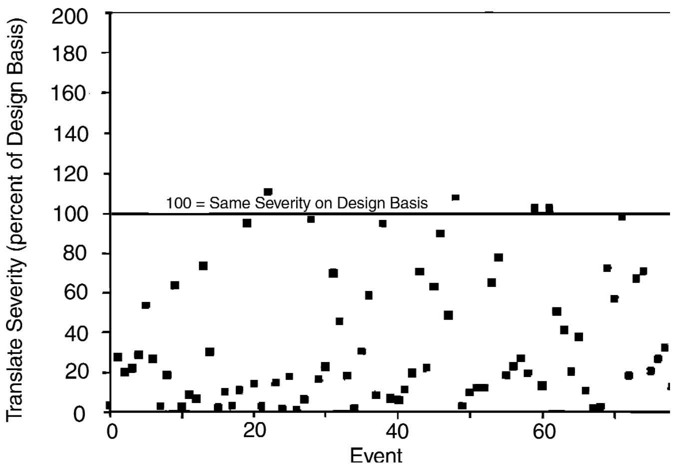

FIG. 41.24 SEVERITY OF TRANSIENT ACTUAL TEMPERATURE CHANGE VERSUS PERCENTAGE OF DESIGN BASIS

steel laboratory specimen could be considerably shorter than that predicted by the Code S-N curves when exposed to high-temperature reactor water. Since then extensive laboratory testing has been conducted both in Japan [95,96] and the United States, principally at Argonne National Laboratory [97,98]. One of the earliest proposed methodologies to incorporate environmental effects in the Code fatigue analyses was the so-called EPRI/GE methodology [99]. This methodology was adopted by the PVRC with some modifications [100] and was forwarded to the BNCS for potential implementation into the ASME Code [101]. The NRC also wrote a letter to the BNCS requesting ASME action to address issues related to the effects of the reactor water environment on the reduction of fatigue life of light-water reactor (LWR) components [102]. In Japan, the Thermal and Nuclear Power Engineering Society (TENPES) Committee for Environmental Fatigue Evaluation Guidelines also has issued a document [103] providing procedures for the evaluation of environmental fatigue effects. Section III has formed a special Task Group to address the issue; the Task Group plans to consider input [100,103] to develop a recommended procedure in the form of a Code Case.

Examples of application of EPRI/GE methodology at critical locations in the RPV and main piping in a BWR have been provided [104,105], as identified elsewhere [106]. The results of environmental fatigue evaluations for one BWR and two PWRs for 60-year operation have been reported [107], and they showed the CUF to be less than 1.0.

Based on the probabilistic analyses and associated sensitivity studies, the NRC concluded that no generic regulatory action was required for the 40-year operating life. However, for the 60-year operation (i.e., an additional 20-year license renewal operation), the Generic Aging Lessons Learned (GALL) Report [108] provides the regulatory guidance to address issues related to metal fatigue of reactor coolant pressure boundary components for license renewal. "The aging management program (AMP) addresses the effects of the coolant environment on component fatigue life by assessing the impact of the reactor coolant environment on a sample of critical components, as a minimum, those components selected in NUREG/CR-6260. The sample of critical components can be evaluated by applying environmental correction factors to the existing ASME Code fatigue analyses. Formulas for calculating the environmental life correction factors are contained in NUREG/CR-6583 for carbon and low-alloy steels and in NUREG/CR-5704 for austenitic stainless steels." The GALL report also lists ten desirable characteristics of an AMP on metal fatigue.

The NCR issued Draft Regulatory Guide DG-1144 [109], later issued as Regulatory Guide 1.207 in March 2007, which includes guidelines for evaluating fatigue analyses incorporating the life reduction of metal components due to the effects of the light water reactor environment for new reactors. The technical basis for the guidelines is contained in NUREG/CR-6909 [110]. The results of the application of DG-1144 guidelines to a BWR feedwater piping system are reported in Reference 111.

41.5.2 Crack Growth Rate Relationships for Fatigue

Fatigue crack growth rates for air environment for austenitic stainless steels is included in ASME BPVC Section XI, Appendix C, and for ferritic materials in Appendix A. Crack growth relationships in the BWR water environment are discussed.

41.5.2.1 Austenitic Stainless Steels. Some of the early fatigue crack growth data in the BWR environment are documented

[112,113]. In 1986, a Section XI task group reviewed the available data for both PWR and BWR environment [78]. It recommended that the fatigue crack growth rate for BWR environment be higher than the air rate by a factor of 10. Argonne researchers have proposed the following relationship of the form [114]:

$$da/dN_{\text{env}} = (da/dN)_{\text{air}} + A(da/dN)_{\text{air}}^{0.5} \tag{12}$$

where $(da/dN)_{\text{air}}$ is that given by the equations in ASME BPVC Section XI, Appendix C. Recently, Argonne researchers have proposed that the first term on the right-hand side of Eq. (12) be multiplied by a factor of two [115]. Japanese researchers also have proposed the following relationship [116]:

$$\begin{aligned} da/dN_{\text{env}} &= (8.17 \times 10^{-12})(T_r^{\,0.5})(\Delta K)^{3.0}/(1 - R)^{2.12} \\ &= (\mathrm{R} > 0,\ 1 \le \Delta K \le 50\ \mathrm{MPa}\sqrt{m}) \end{aligned} \tag{13}$$

where, da/dN is in m/cycle, T_r is the rise time in seconds, and ΔK is in MPa $\sqrt{\mathrm{m}}$. T_r should be assumed to be 1 sec when rise time is less than 1 sec; T_r should be assumed to be 1,000 seconds if rise time is unknown. This relationship has been incorporated in the draft Japan Maintenance Standard [117].

An EPRI-funded effort [118] is currently underway to review the available literature to develop austenitic stainless steel fatigue crack growth relationships in a water environment for inclusion in ASME BPVC Section XI, Appendix C. It may be noted that the fatigue crack growth is typically insignificant compared to SCC growth rate in the evaluation of cracked stainless steel components subjected to a BWR water environment.

41.5.2.2 Ferritic Steels. ASME BPVC Section XI, Appendix A, contains the environmental fatigue crack growth rates. These relationships are presently used in BWR applications such as the fracture mechanics evaluation of postulated nozzle corner crack. Based on more recent data on the LWR environment, a new rise-time-based model has been proposed [119]. Based on this work and the work by James [120] on conditions that lead to the initiation and cessation of environmentally assisted crack growth, Code Case N-643 [121] has been developed for PWR applications.

Some recent data [122] indicate that, under certain conditions (such as very high R-ratio and long rise time), environmentally assisted fatigue crack growth under a BWR environment could be significantly higher than that predicted by the current ASME BPVC Section XI, Appendix A curves (see Fig. 41.25). A review of available relevant BWR data is in progress under a joint EPRI/GE-sponsored program; the outcome of this program is expected to be a proposed Code Case, similar to Code Case N-643, applicable to BWR environments.

41.5.3 Crack Growth Rate Relationships for SCC

Key drivers in the crack growth rate due to SCC are the sustained stresses that include not only the externally applied stresses but also residual stresses from sources such as welding. Therefore, the crack growth rate relationships are of the following form:

$$da/dt = \mathrm{C}(K)^{\mathrm{n}} \tag{14}$$

where C and n are constants dependent on material and environmental conditions. ASME BPVC Section XI does not provide any guidance in this area. Efforts are currently underway in the Working Group on Flaw Evaluation to review the available information and develop SCC growth rate relationship for incorporation into ASME BPVC Section XI. The BWR Owners have generally used the NRC-approved bounding crack growth rates for flaw evaluation purposes (e.g., see discussion in para. 41.2.2.1 regarding shroud). For piping, NUREG-0313, Revision 2 [9] provides crack growth rate relationship in the Eq. (14) format. Some of the other available BWR SCC growth rate correlations are reviewed.

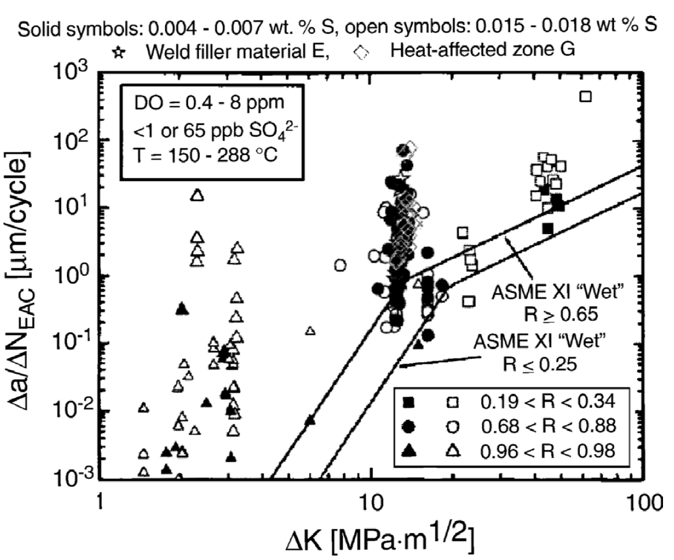

FIG. 41.25 EFFECT OF LOADING CONDITIONS ON $\Delta a/\Delta N_{EAC}$ AND COMPARISON WITH ASME SECTION XI CURVES

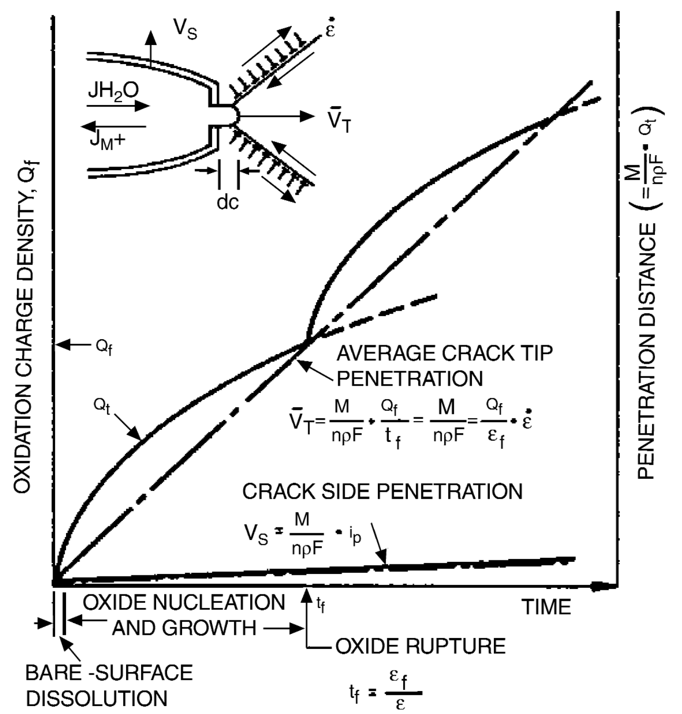

FIG. 41.26 SCHEMATIC OXIDATION CHARGE DENSITY/TIME RELATIONSHIP FOR A STRAINED CRACK TIP AND UNSTRAINED CRACK SIDES

41.5.3.1 Austenitic and Nickel-Based Materials. A crack growth rate prediction model based on slip dissolution/film rupture mechanism [123] has correlated well with the measured crack growth rates in widely varying BWR environmental conditions (e.g., NWC and HWC). In this model (Fig. 41.26), crack advance is related to the oxidation reactions that occur at the crack tip as the protective film is ruptured by increasing strain in the underlying matrix. This rupture event occurs with a periodicity, t_f, which is determined by the fracture strain of the oxide and the strain rate at the crack tip. The extent of the crack advance is related by Faraday's Law to the oxidation charge density associated with dissolution and oxide growth (passivation) on the bare metal surface, as represented in Fig. 41.26. These relations vary with time in a complex manner for different environment and material chemistries; however, the resultant growth rate, V_T, relationship shown in Fig. 41.26 can be restated in a general form as follows:

$$V_T = f(n)(\varepsilon_{ct})^n \tag{15}$$

where ε_{ct}', the crack tip strain rate, embodies the mechanical contributions and n is a parameter that represents the effects of the environment (ECP, water conductivity) and material chemistries (EPR, a measure of sensitization of stainless steel) on environmentally assisted crack growth. For NWC conditions (conductivity = 0.1 μS/cm, ECP = 200 mV), and EPR = 15.0 (weld-sensitized condition), $n = 0.61$ and the crack growth rate relationship is the following:

$$da/dt = 2.93 \times 10^{-07} K^{2.455} \tag{16}$$

For HWC conditions (conductivity = 0.1 μS/cm, ECP = −230 mV), and EPR = 15.0 (weld-sensitized condition), $n = 0.97$ and the crack growth rate relationship is the following:

$$da/dt = 2.53 \times 10^{-11} K^{3.884} \tag{17}$$

where

da/dt = crack growth rate in mm/hr
K = sustained stress intensity factor, MPa $\sqrt{m}$

The BWRVIP has also developed an SCC growth rate relationship for use by the participating members [124] and represented by the following:

$$Ln(da/dt) = C_1[ln(K)] - C_2(Cond)^m + C_3(ECP) + C_4/T_{ABS} - C_5 \tag{18}$$

where

da/dt = crack growth rate
K = sustained stress intensity factor
$Cond$ = water conductivity
T_{ABS} = temperature, °K
C_1, C_2, C_3, C_4, C_5, and m are constants

For BWR NWC conditions, the appropriate values are as follows $Cond$ = 0.1 μS/cm, ECP = 200 mV (SHE), and T_{ABS} = temperature, °K, = 561°K (= 550°F). Using a specified factor of 10.3 to obtain 95th percentile curve, the relationship is the following:

$$da/dt = 2.135 \times 10^{-07} K^{2.181} \tag{19}$$

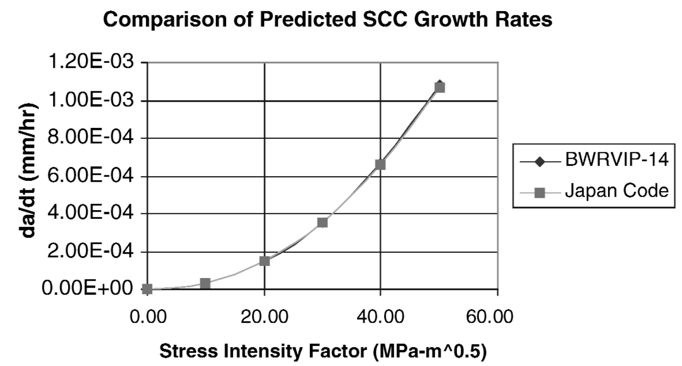

FIG. 41.27 COMPARISON OF BWRVIP-14 AND JAPAN MAINTENANCE CODE PREDICTIONS

The units of da/dt and K are the same as those in Eq. (17). The draft Japan Maintenance Standard [117] provides the following crack growth rate relationship for BWR NWC conditions [units the same as in Eq. (19)]:

$$da/dt = 2.27 \times 10^{-07} K^{2.161} \tag{20}$$

Figure 41.27, [125] shows a comparison of the predictions of Eqs. (19) and (20). It is seen that the crack growth predictions based on the BWRVIP and draft Japan Maintenance Standard are very close. However, the factors of reduction in crack growth rate in going from NWC to HWC are different. The BWRVIP correlation predicts a reduction factor of 4.7 and the draft Maintenance Standard allows a factor of 7.9. The NRC has, however, allowed only a credit of factor of 2 in BWR flaw evaluations [126].

For the nickel-based alloys (such as alloy 600, weld metals alloys 182 and 82), several relationships have been proposed. The relationships based on the film/rupture model have been given [127], including the BWRVIP-59 relationships [125]. Lastly, the crack growth relationships proposed by the Argonne researchers have also been described [115].

41.5.3.2 Ferritic Steels. ASME BPVC Section XI does not contain SCC growth rate relationship for the ferritic materials in BWR environment. Reference 128 provides an assessment of SCC crack growth rate algorithms for low alloy steels under BWR conditions. Figure 41.28 shows the BWRVIP-proposed relationship [122]. The basic crack growth rate is 2×10^{-11} mm/sec. The DL2 line is given by the following:

$$da/dt = 3.29 \times 10^{-14} (K)^4 \tag{21}$$

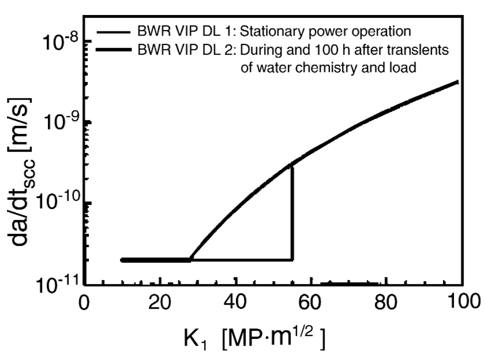

FIG. 41.28 BWRVIP-60 SCC DISPOSITION LINES

where K is in MPa$\sqrt{m}$ and the crack growth rate is in mm/sec. The vertical line in Fig. 41.28 is at 55 MPa$\sqrt{m}$.

Field experience [129,52] has shown that even when SCC initiated in the cladding, the cracks did not progress into the low-alloy steel base metal or beyond HAZ. However, the proposed BWRVIP relationship was used in flaw evaluation [52].

The data that formed the basis of the BWRVIP SCC relationship and the fatigue crack growth rate data, such as that shown in Fig. 41.25, will be reviewed as a part of a joint EPRI/GE project discussed in para. 41.5.2.2.

41.5.4 Crack Growth Rate Monitoring

Online monitoring of crack growth rates on a fracture mechanics specimen under actual reactor environment may provide extra confidence in the crack growth rate used in the flaw evaluation. One such monitoring system is called crack arrest/advance verification system (CAVS); an example of the successful application of CAVS for monitoring crack indications in the recirculation inlet safe end at an operating BWR has been presented [130]. Use of CAVS confirmed the benefit of water chemistry improvements implemented at this plant and, subsequently, led to the elimination of a special midcycle UT examination required by the NRC.

During a routine scheduled ISI, UT indications were discovered in certain recirculation inlet safe ends at an operating BWR plant. The indications were located in the region of the thermal sleeve to safe-end weld. Since immediate replacement of the safe end would have caused an unanticipated extended outage and very high costs, a fracture mechanics crack growth analysis was performed to demonstrate that continued operation for the next fuel cycle could be justified while maintaining acceptable structural margins required by ASME BPVC Section XI. The analysis considered the indication in the limiting safe end and assumed conservative residual stresses for crack growth analysis. Also, the plant owner agreed to complete the maintenance of plant chemical equipment and to implement improved water quality procedure, along with the installation of CAVS, to monitor the expected improvements in crack growth during the following operating cycle. Although the NRC accepted the technical arguments concerning structural integrity, they also requested a midcycle UT to provide further assurance that sufficient structural margins were being maintained.

The CAVS installed at the plant consisted of a crack growth monitor and a water quality module. The crack growth monitor used reversing DC potential technology for accurate measurement of the growth of pre-existing cracks in fracture mechanics specimens. The water chemistry module monitored the bulk water chemistry (dissolved oxygen, pH, conductivity, and ECP) of the water being supplied to CAVS; 1 in. thick compact tension specimens with heat treatment similar to that of the safe end were tested in an autoclave connected to the reactor recirculation line. Because CAVS used the actual plant recirculation water, the crack growth specimens were subjected to the same water chemistry exposure as recirculation safe ends and piping.

Figure 41.29 shows typical results from CAVS for a 304 stainless steel specimen. It is seen that the monitoring system is extremely sensitive and that the observed crack growth rates correlate with conductivity [i.e., the crack growth rate is higher when the conductivity is high over a period of time (such as during startup) and is lower when the average conductivity is lower]. Using the CAVS specimen data, plant-specific growth rates were established and used to predict crack growth in the safe end (Fig. 41.30). It is seen that the CAVS growth prediction was well

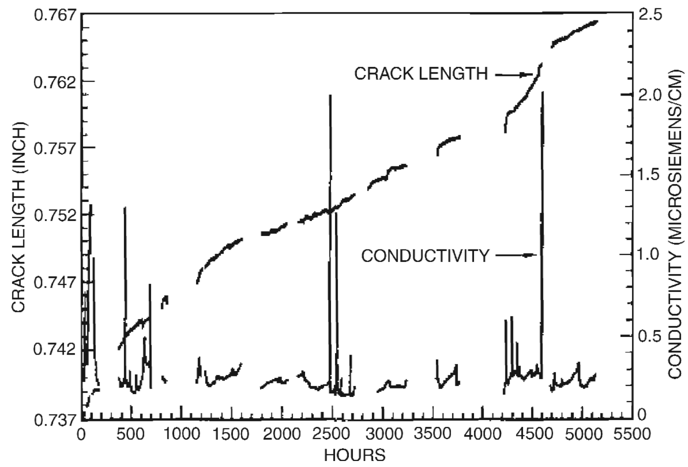

FIG. 41.29 CRACK LENGTH VERSUS TOTAL TIME-ON-TEST FOR TYPE 304 STAINLESS STEEL

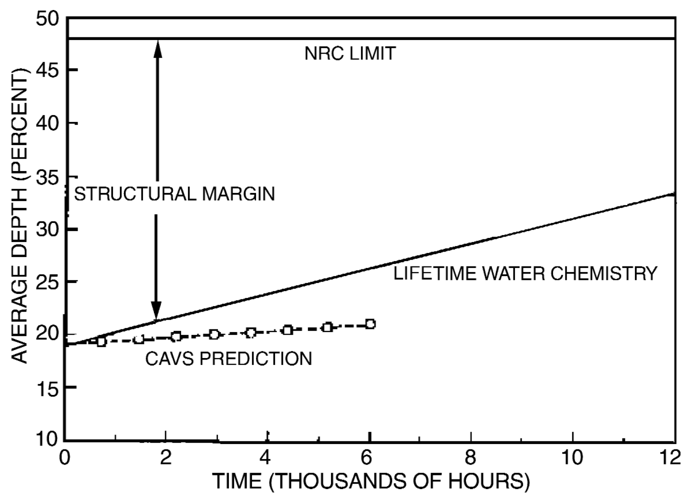

FIG. 41.30 PREDICTED CRACK GROWTH IN SAFE END

below the bounding crack growth evaluation based on plant water chemistry history. In turn, the final crack depth at the end of the fuel cycle was well below the allowable depth based on providing the nominal ASME Code margin of 3 on stress and an additional factor of 1.5 on crack depth imposed by the NRC. These results confirmed that sufficient structural margins were maintained and that a special midcycle examination was unnecessary. The NRC concurred, and the midcycle inspection requirement was eliminated.

41.6 SUMMARY

A review of the applications of many and sometimes unique ways in which the provisions of ASME BPVC Sections III and XI have been used in addressing the service-induced degradation in the BWR vessels, internals, and pressure boundary piping. The vessel internals addressed included steam dryer, shroud, and jet pumps. The vessel components considered were feedwater nozzle, stub tube welds, and attachment and shroud support welds. A review of pressure boundary piping flaw evaluation methods also included consideration of weld overlay repairs. The service-related degradation mechanisms considered were environmental fatigue crack initiation and growth and stress corrosion cracking.

41.7 REFERENCES

1. U.S. NRC Information Notice 2002–26, Failure of Steam Dryer Cover Plate After a Recent Power Uprate (with Supplements 1 and 2). Washington, DC: U.S. Nuclear Regulatory Commission; 2002, 2003, 2004.
2. Alexander JE, et al. Alternate Alloys for BWR Piping Applications (EPRI NP-2671-LD). Palo Alto, CA: Electric Power Research Institute; 1982.
3. Horn RM, et al. Experience and Assessment of Stress Corrosion Cracking in L-Grade Stainless Steel BWR Internals. *Nuclear Engineering and Design* 1997;174:313–325.
4. Hedden O. Overview of Section XI Stipulations (para. 26.5.2). In: *Companion Guide to the ASME Boiler & Pressure Vessel Code*. New York: American Society of Mechanical Engineers; 2006.
5. Bilanin W, Dyle R. Boiling Water Reactor and Internals Project Overview. ANS Transaction.
6. Wagoner V, Mulford T. The BWR Vessel and Internals Project - 2001 and Beyond. Proceedings of International Conference on Nuclear Engineering (ICONE-9). 2001.
7. 7 Dyle R, Mulford T, Bilanin W. BWR Vessel and Internals Project Elements Applicable to Advanced Nuclear Plants. Proceedings of International Congress on Advances in Nuclear Power Plants (ICAPP03). Cardoba, Spain; 2003.
8. BWR Core Shroud Inspection and Flaw Evaluation Guidelines (BWRVIP-01, Revision 2). 1996.
9. Technical Report on Material Selection and Processing Guidelines for BWR Coolant Pressure Boundary Piping (NUREG-0313, Revision 2). Washington, DC: U.S. Nuclear Regulatory Commission; 1988.
10. Resolution of Core Shroud Cracking at Dresden Unit 3, and Quad Cities, Unit 1 (TAC M89871/TAC M89493). Washington, DC: U.S. Nuclear Regulatory Commission; 1994.
11. BWRVIP-14, BWR Vessel and Internals Project, Evaluation of Crack Growth in BWR Stainless Steel Internals (EPRI Report TR-105873). Palo Alto, CA: Electric Power Research Institute; 1996.
12. Final Safety Evaluation of Proprietary Report TR-105873, BWR Vessel and Internals Project, Evaluation of Crack Growth in BWR Stainless Steel Internals (BWRVIP-14). (TAC M94975) December 3, 1999.
13. Mehta HS, Inch G, Dhar S. A Fracture Mechanics Evaluation of BWR Shroud Mid-Core Horizontal Weld to Justify Continued Operation. In: ASME PVP Vol. 463, *Flaw Evaluation, Service Experience, and Reliability.* New York: American Society of Mechanical Engineers; 2003; pp. 178–190.
14. BWRVIP-99, BWR Vessel and Internals Project, Crack Growth Rates in Irradiated Stainless Steels in BWR Internal Components. Palo Alto, CA: Electric Power Research Institute; 2001.
15. BWRVIP-03, Revision 1, Reactor Pressure Vessel and Internals Examination Guidelines (EPRI Report TR-105696). Palo Alto, CA: Electric Power Research Institute; 1999.
16. Design Criteria for Irradiated Type-304 Stainless Steel in BWR Applications (GE Report NEDE-20364); 1974.
17. Evaluation of BWR Top-Guide Integrity (EPRI Report NP-4767). Palo Alto, CA: Electric Power Research Institute; 1986.
18. Clarke WL, White MA, Ranganath S. Evaluation of the Fracture Toughness of Irradiated Stainless Steel Using Short Rod Specimens (ASTM STP 1046). West Conshohocken, PA: American Society for Testing and Materials; 1990; pp. 470–486.
19. Herrera ML, Ranganath S. Fracture Toughness Assessment of Irradiated Core Support Structures in a Boiling Water Reactor. Postconference Seminar 2, 11th International Conference on Structural Mechanics in Reactor Technology; Taipei, Taiwan; 1991.
20. Herrera ML, et al. Evaluation of the Effects of Irradiation on the Fracture Toughness of BWR Internal Components, 4th International Conference on Nuclear Engineering, Vol. 5. New York: American Society of Mechanical Engineers; 1996.
21. Fracture Toughness and Crack Growth Rates of Irradiated Austenitic Stainless Steels (NUREG/CR-6826). Washington, DC: U.S. Nuclear Regulatory Commission; 2003.
22. BWRVIP-100, BWR Vessel and Internals Project, Updated Assessment of the Fracture Toughness of Irradiated Stainless Steel for BWR Core Shrouds. Palo Alto, CA: Electric Power Research Institute; 2001.
23. Carpenter M, et al. Boiling Water Reactor Core Shroud Repair. *Nuclear Plant Journal* May-June 1995.
24. Arai T, et al. BWR Core Internals Replacement. *Nuclear Engineering and Design* 2000;198:165–171.
25. Mehta HS. A Fracture Mechanics Evaluation of Service-Induced Flaws at Jet Pump Riser Elbow Welds. In: ASME PVP Vol. 410-2, *Assessment Methodologies for Preventing Failure.* New York: American Society of Mechanical Engineers; 2000; pp. 119–125.
26. Liaw PK, Peck MG, Mehta HS. Fatigue Crack Propagation Behavior of Stainless Steels. GE Nuclear Energy Report, Contract 52988B860X; 1990 .
27. Zahoor A. Ductile Fracture Handbook (EPRI Report NP-6301-D). Palo Alto, CA: Electric Power Research Institute; 1989.
28. GE Service Information Letter 644, Supplement 1, BWR Steam Dryer Integrity; September 5, 2003.
29. BWRVIP-139: BWR Vessel and Internals Project, Steam Dryer Inspection and Flaw Evaluation Guidelines, EPRI, Palo Alto, CA, 2005. 1011463
30. Ranganath S, Chapman TL. Inservice Inspection Experience in Boiling Water Reactors. *Nuclear Plant Journal* 1992;77–80.
31. BWR Vessel and Internals Project, BWR Reactor Pressure Vessel Shell Weld Inspection Recommendations (BWRVIP-05). September 28, 1995.
32. Final Safety Evaluation of the BWR Vessel and Internals Project BWRVIP-05 Report (TAC No. M93925), U.S. Nuclear Regulatory Commission letter, 1998.
33. Elliot BJ, et al. Risk-Informed Assessment of Inservice Inspection of Reactor Pressure Vessel Welds in Boiling Water Reactors. In: ASME PVP-Vol. 392, *Service Experience in Fossil and Nuclear Power Plants.* New York: American Society of Mechanical Engineers; 1999; pp. 173–180.

34 Yao D, et al. Reactor Vessel Cold Overpressure Event for Kuosheng Nuclear Station Unit 1 During EOC-6 Refueling Outage. First JSME/ASME International Conference on Nuclear Engineering, Vol. 2. 1991.

35. Herrera ML, et al. Application of Probabilistic Fracture Mechanics Methods to Evaluate Boiling Water Reactor Pressure Vessel

Integrity. Proceedings of 8th International Conference on Nuclear Engineering (ICONE-8). 2000.

36. U.S. NRC BWR Feedwater Nozzle and Control Rod Drive Return Line Nozzle Cracking Report (NUREG-0619). Washington, DC: U.S. Nuclear Regulatory Commission; 1980.

37. Boiling Water Reactor Feedwater Nozzle/Sparger Final Report, GE Report NEDO-21821-A, February 1980.

38. Alternate BWR Feedwater Nozzle Inspection Requirements, Report GE-NE-523-A71-0594-A, Revision 1, May 2000.

39. U.S. NRC BWROG – Safety Evaluation of Proposed Alternative to BWR Feedwater Nozzle Inspections (TAC M94090). Washington, DC: U.S. Nuclear Regulatory Commission; 1998.

40. ASME BPVC Code Case N-648-1, Alternative Requirements for Inner Radius Examinations of Class 1 Reactor Vessel Nozzles, Section XI, Division 1. In: *ASME Boiler and Pressure Vessel Code.* New York: American Society of Mechanical Engineers.

41. Bamford WH, et al. Technical Basis for Elimination of Reactor Pressure Vessel Nozzle Inner Radius Inspections (PVP Vol. 422). New York: American Society of Mechanical Engineers; 2001.

42. U.S. NRC Regulatory Guide 1.147, Inservice Inspection Code Case Acceptability, ASME Section XI, Division 1 (Revision 13). Washington, DC: U.S. Nuclear Regulatory Commission; 2003.

43. ASME BPVC Code Case N-702, Alternative Requirements for Boiling Water Reactor (BWR) Nozzle Inner Radius and Nozzle-to-Shell Welds, Section XI, Division 1. In: *ASME Boiler and Pressure Vessel Code.* New York: American Society of Mechanical Engineers.

44. BWRVIP-108, BWR Vessel and Internals Project, Technical Basis for the Reduction of Inspection Requirements for the Boiling Water Reactor Nozzle-to-Shell Welds and Nozzle Blend Radii (EPRI Technical Report 1003557). Palo Alto, CA: Electric Power Research Institute; 2002.

45. U.S. NRC Safety Evaluation, Oyster Creek Nuclear Generating Station – Alternative Repair of Control Rod Drive Housing Interface With Reactor Vessel (TAC MB5700). Washington, DC: U.S. Nuclear Regulatory Commission; 2002.

46 ASME BPVC Code Case N-730, “Roll Expansion of Class 1 Control Rod Drive Bottom Head Penetrations in BWRs,” approved October 4, 2006.

47. BWRVIP-146: BWR Vesel and Internals Project, Technical Basis for ASME Code Case N-730, “Roll Expansion of Class 1 Control Rod Drive Bottom Head Penetrations in BWRs,” EPRI, Palo Alto, CA: 2005. 1011690.

48. BWRVIP-17, BWR Vessel and Internals Project, Roll/Expansion Repair of Control Rod Drive and In-Core Instrument Penetrations in BWR Vessels (EPRI Technical Report TR-106712). Palo Alto, CA: Electric Power Research Institute; 1996.

49. Ranganath S, et al. Proactive Approaches to Assure the Structural Integrity of Boiling Water Reactor Components. *Nuclear Engineering and Design* 1990;124:53–70.

50. ASME BPVC Code Case N-606-1, Similar and Dissimilar Welding Using Ambient Temperature Machine GTAW Temper Bead Technique for BWR CRD Housing/Stub Tube Repairs, Section XI, Division 1. In: *ASME Boiler and Pressure Vessel Code.* New York: American Society of Mechanical Engineers.

51. GE Service Information Letter 624, Stress Corrosion Cracking in Alloy 182 Welds in Shroud Support Structure. March 24, 2000.

52. Mehta HS, Horn RM, Inch G. A Fracture Mechanics Evaluation of Observed Cracking at a BWR-2 Reactor Pressure Vessel Weld. In: ASME PVP-Vol. 437, *Service Experience and Failure Assessment Applications.* New York: American Society of Mechanical Engineers; 2002; pp. 153–164.

53. BWRVIP-60, BWR Vessel and Internals Project, Evaluation of Stress Corrosion Crack Growth in Low Alloy Steel Vessel Materials in the BWR Environment (EPRI TR-108709). Palo Alto, CA: Electric Power Research Institute; 1999.

54. Gordon BM, et al. Service Experience of BWR Pressure Vessels. In: *Performance and Evaluation of Light Water Reactor Pressure Vessels* (ASME PVP-Vol. 119). New York: American Society of Mechanical Engineers; 1987; pp. 9–17.

55. CFR Title 10, Part 50, Appendix G, Fracture Toughness Requirements. In: *Code of Federal Regulations.* Washington, DC: National Archives and Records Administration’s (NARA) Office of the Federal Register (OFR)/Government Printing Office (GPO); 2005.

56. U.S. NRC Radiation Embrittlement of Reactor Vessel Materials (Regulatory Guide 1.99, Revision 2). Washington, DC: U.S. Nuclear Regulatory Commission; 1988.

57. Johnson R. Resolution of the Reactor Vessel Materials Toughness Safety Issue, Volumes 1 and 2 (NUREG 0744). Washington, DC: U.S. Nuclear Regulatory Commission; 1982.

58. WRC Bulletin 413, Development of Criteria for Assessment of Reactor Vessels With Low Upper-Shelf Fracture Toughness. New York: Welding Research Council; 1996.

59. ASME BPVC Code Case N-512, Assessment of Reactor Vessels with Low Upper Shelf Charpy Impact Energy Levels, Section XI, Division 1. In: *ASME Boiler and Pressure Vessel Code.* New York: American Society of Mechanical Engineers.

60. U.S. NRC Regulatory Guide 1.161, Evaluation of Reactor Pressure Vessels with Charpy Upper-Shelf Energy Less Than 50 ft-lb. Washington, DC: U.S. Nuclear Regulatory Commission; 1995.

61. Mehta HS, et al. 10 CFR50 Appendix G Equivalent Margin Analysis for Low Upper Shelf Energy in BWR/2 Through BWR/6 Vessels (NEDO-32205, Revision 1, Licensing Topical Report for BWR Owners’ Group). 1993.

62. U.S. NRC Safety Evaluation by the Office of Nuclear Reactor Regulation – BWR Owners’ Group Topical Report NEDO-32205, Revision 1 on Upper Shelf Energy Equivalent Margin Analysis. Washington, DC: U.S. Nuclear Regulatory Commission; 1993.

63. Klepfer HH, et al. Investigation of Cause of Cracking in Austenitic Stainless Steel Piping (GE Report NEDO-21000). 1975.

64. U.S. NRC Investigation and Evaluation of Stress-Corrosion Cracking in Piping of Light Water Reactor Plants (NUREG-0531). Washington, DC: U.S. Nuclear Regulatory Commission; 1979.

65. U.S. NRC Report of the Piping Review Committee (NUREG-1061). Washington, DC: U.S. Nuclear Regulatory Commission; 1984.

66. BWR Owners Group IGSCC Research Program, Executive Summary 1979-1983 (EPRI Report NP-4273-SR). Palo Alto, CA: Electric Power Research Institute; 1985.

67. BWR Owners Group IGSCC Research Program, Executive Summary 1984-1988 (EPRI Report NP-6927-D). Palo Alto, CA: Electric Power Research Institute; 1990.

68. Jones RL, et al. Controlling Stress Corrosion Cracking in Boiling Water Reactors. *Nuclear Engineering and Design* 1993;143: 111– 123.

69. Porowski JS, et al. Use of Mechanical Stress Improvement Process to Mitigate Stress Corrosion Cracking in BWR Piping Systems. *Nuclear Engineering and Design* 1990;124:91–100.

70. Smith RE, et al. Pressure Vessel Nozzle Repair. *Nuclear Engineering and Design* 1990;124:79–89.

71. Evaluation of Safe-End Weld Materials and Safe End Replacement Experience (EPRI Report NP-4443). Palo Alto, CA: Electric Power Research Institute; 1986.

72. Riccardella PC, et al. Weld Overlay Repairs from Conception to Long-Term Qualification. *International Journal of Pressure Vessels and Piping* 1988;34:59–82.

73. Continued Service Justification for Weld Overlay Pipe Repairs. Final Draft Report prepared for BWR Owners Group Pipe Cracking Program and EPRI, May 1984.

74. Mehta HS. J-Integral Analysis of Ductile Fracture Margin in Piping Weld Overlays. *Transactions of the Ninth International Conference on Structural Mechanics in Reactor Technology* 1987;G:469–474.

75. Justification for Extended Weld-Overlay Design Life (EPRI Report NP-7103-D). Palo Alto, CA: Electric Power Research Institute; 1991.

76. ASME BPVC Code Case N-504, Alternative Rules for Repair of Classes 1, 2, and 3 Austenitic Stainless Steel Piping. In: *ASME Boiler and Pressure Vessel Code.* New York: American Society of Mechanical Engineers.

77. Ranganath S, Mehta HS. Engineering Methods for the Assessment of Ductile Fracture Margin in Nuclear Power Plant Piping. *Elastic-Plastic Fracture: Second Symposium, Volume II – Fracture Resistance Curves and Engineering Applicati*ons (ASTM Special Technical Publication 803). West Conshohocken, PA: American Society for Testing and Materials; 1981.

78. Evaluation of Flaws in Austenitic Steel Piping. *Journal of Pressure Vessel Technology* 1986;108:352-366.

79. Assessment of Design Basis for Load-Carrying Capacity of Weld-Overlay Repairs (NUREG/CR-4877). Washington, DC: U.S. Nuclear Regulatory Commission; 1987.

80. Kulat SD, et al. Experimental Verification of Analytically Determined Weld Overlay Residual Stress Distribution. Eighth International Conference on Structural Mechanics in Reactor Technology, August 1985.

81. Non-Mandatory Appendix Q, ASME Section XI, "Weld Overlay Repair of Classes 1, 2, and 3 Austenitic Stainless Steel Piping Weldments."

82. Inconel Weld Overlay Repair for Low-Alloy Steel Nozzle to Safe-End Joint (EPRI Report NP-7085-D). Palo Alto, CA: Electric Power Research Institute; 1991.

83. ASME BPVC Code Case N-432, Repair Welding Using Automatic or Machine Gas Tungsten-Arc Welding (GTAW) Temper Bead Technique, Section XI, Division 1. In: *ASME Boiler and Pressure Vessel Code.* New York: American Society of Mechanical Engineers.

84. ASME BPVC Code Case N-638, Similar and Dissimilar Metal Welding Using Ambient Temperature Machine GTAW Temper Bead Technique, Section XI, Division 1. In: *ASME Boiler and Pressure Vessel Code.* New York: American Society of Mechanical Engineers.

85. ASME BPVC Code Case N-740, "Dissimilar Metal Weld Overlay for Repair of Class 1, 2, and 3 Items, Approved October 12, 2006.

86. Cipolla RC, Scarth DA, Wilkowski GM, Zilberstein VA. Technical Basis for Proposed Revision to Acceptance Criteria for ASME Section XI Pipe Flaw Evaluation (ASME PVP Vol. 422). New York: American Society of Mechanical Engineers; 2001: pp. 31–51.

87. Mehta HS. Weld Overlay Design Calculations Using the Current and Proposed IWB-3640 Procedures. General Electric Co. unpublished work for the ASME Section XI Working Group on Pipe Flaw Evaluation; 2001.

88. Scarth DA, et al. Flaw Evaluation Procedures and Acceptance Criteria for Nuclear Piping in ASME Code Section XI (ASME PVP Vol. 463). New York: American Society of Mechanical Engineers; 2003: pp. 45–61.

89. Mehta, H.S. A Review of Fatigue & SCC Crack Growth Rate Relationships for Ferritic & Stainless Steels and Ni-Cr-Fe Materials in BWR Water Environment, Proceedigs of ASME PVP 2006-ICPVT-11, Paper # PVP2006-ICPVT11-93853.

90. Cooper WE. The Initial Scope and Intent of the Section III Fatigue Design Procedures. PVRC Workshop on Environmental Effects on Fatigue Performance, Clearwater Beach, FL, January 20, 1992, pp. 1–6.

91. Stevens GL, Ranganath S. Use of On-Line Fatigue Monitoring of Nuclear Reactor Components as a Tool for Plant Life Extension. *Journal of Pressure Vessel Technology* 1991;113:349–357.

92. Sakai T, et al. Implementation of Automated, On-Line Fatigue Monitoring in a Boiling Water Reactor (ASME PVP Vol. 252). New York: American Society of Mechanical Engineers; 1993: pp. 67–74.

93. Stevens GL, et al. Fatigue Monitoring for Demonstrating Fatigue Design Basis Compliance (ASME PVP Vol. 383). New York: American Society of Mechanical Engineers; 1999: pp. 111–116.

94. Higuchi M, Iida K. Fatigue Strength Correction Factors for Carbon and Low-Alloy-Steels in Oxygen-Containing High-Temperature Water. *Nuclear Engineering and Design* 1991;129:293–306.

95. Higuchi M. Fatigue Curves and Fatigue Design Criteria for Carbon and Low-Alloy Steels in High-Temperature Water (ASME PVP Vol. 386). New York: American Society of Mechanical Engineers; 1999: pp. 161–169.

96. Higuchi M, Iida K. Reduction in Low-Cycle Fatigue Life of Austenitic Stainless Steels in High Temperature Water (ASME PVP Vol. 353). New York: American Society of Mechanical Engineers; 1997: pp. 79–85.

97. Chopra OK, Shack WJ. Effects of LWR Coolant Environments on Fatigue Design Curves of Carbon and Low-Alloy Steels (NUREG/CR-6583). Washington, DC: U.S. Nuclear Regulatory Commission; 1998.

98. Chopra OK. Effects of LWR Coolant Environments on Fatigue Design Curves of Austenitic Stainless Steels (NUREG/CR-5704). Washington, DC: U.S. Nuclear Regulatory Commission; 1999.

99. Mehta HS, Gosselin SR. Environmental Factor Approach to Account for Water Effects in Pressure Vessel and Piping Fatigue Evaluations. *Nuclear Engineering and Design* 1998;181: 175–197.

100. Mehta HS. An Update on the Consideration of Reactor Water Effects in Code Fatigue Initiation Evaluations for Pressure Vessels and Piping (ASME PVP Vol. 410-2). New York: American Society of Mechanical Engineers; 2000: pp. 45–51.

101. Hollinger GL. Executive Director, PVRC, Letter to J.H. Ferguson, Chairman, BNCS, October 31, 1999.

102. Craig JW. Director, Division of Engineering Technology, Office of Nuclear Regulatory Research, U.S. Nuclear Regulatory Commission, Letter to J.H. Ferguson, Chairman, BNCS, December 1, 1999.

103. Guidelines on Environmental Fatigue Evaluation for LWR Component. Japan: Thermal and Nuclear Power Engineering Society; 2002 (English translation).

104. Mehta HS. Application of EPRI/GE Environmental Factor Approach to Representative BWR Pressure Vessel and Piping Fatigue Evaluations (ASME PVP Vol. 360). New York: American Society of Mechanical Engineers; 1998: pp. 413–425.

105. Evaluation of Environmental Thermal Fatigue Effects on Selected Components in a Boiling Water Reactor Plant (EPRI Report TR110356). Palo Alto, CA: Electric Power Research Institute; 1998.

106. Ware AG, et al. Application of NUREG/CR-5999 Interim fatigue Curves to Selected Nuclear Power Plant Components (NUREG/CR6260). Washington, DC: U.S. Nuclear Regulatory Commission; 1995.

107. Ohata H, et al. Environmental Fatigue Evaluation on Japanese Nuclear Power Plants (ASME PVP Vol. 410-2). New York: American Society of Mechanical Engineers; 2000: pp. 79–84.

108. Generic Aging Lessons Learned (GALL) Report: Appendix X.M1, Metal Fatigue of Reactor Coolant Pressure Boundary (NUREG1801, Volume 1). Washington, DC: U.S. Nuclear Regulatory Commission; 2001.

109 Draft Regulatory Guide DG-1144: Guidelines for Evaluating Fatigue Analyses Incorporating the Life Reduction of Metal Components Due to the Effects of the Light Water Reactor Environment for New Reactors; US Nuclear Regulatory Commission, July 2006.

110. Chopra, O.K. and W.J. Shack, “Effects of LWR Coolant Environments on the Fatigue Life of Reactor Materials,” NUREG/CR-6909, Draft Report, February 2006; Final Report February 2007.

111. Mehta, H.S. and H.L. Hwang, “Application of Draft Regulatory Guide DG-1144 Guidelines for Environmental fatigue Evaluation to a BWR feedwater Piping System,” Proceedings of ASME-PVP 2007, Paper No. PVP2007-26143.

112. Hale DA, et al. Fatigue Crack Growth in Piping and RPV Steels in Simulated BWR Water Environment (GE Report GEAP-24098, prepared for U.S. Nuclear Regulatory Commission). 1978.

113. Kawakubo T, et al. Crack Growth Behavior of Type 304 Stainless Steel in Oxygenated 290C Pure Water Under Low Cyclic Frequency Loading. *Corrosion* 1980;36:638-647.

114. Review of Environmental Effects on Fatigue Crack Growth of Austenitic Stainless Steels (NUREG/CR-6176). Washington, DC: U.S. Nuclear Regulatory Commission; 1994.

115. Chopra OK, Shack W. Crack Growth Rates in Austenitic Stainless Steels and Ni-Alloys in LWR Environments. Proceedings of Workshop on Flaw Growth in Austenitic and Nickel Based Materials, August 1, 2002, Snowbird, Utah.

116. Itatani M, et al. Fatigue Crack Growth Curve for Austenitic Stainless Steels in BWR Environment. *Journal of Pressure Vessel Technology* 2001;123:166–172.

117. Honjin M, Hasegawa K, Iida K. Items Concerned with Flaw Evaluation in a Draft of New Maintenance Standards for LWR in Japan. Presentation at Section XI S/G Evaluation Standards Meeting, Lake Buena Vista, FL, August 12, 1998.

118. Cipolla RC. Overview of ASME Section XI Needs. Proceedings of Workshop on Flaw Growth in Austenitic and Nickel Based Materials, August 1, 2002, Snowbird, Utah.

119. WRC Bulletin 404, Fatigue Crack Growth of Low-Alloy Steels in Light Water Reactor Environments. New York: Welding Research Council; 1995.

120. James LA. Technical Basis for the Initiation and Cessation of Environmentally Assisted Cracking of Low-Alloy Steels in Elevated Temperature PWR Environments (ASME PVP Vol. 374). New York: American Society of Mechanical Engineers; 1998: pp. 207–230.

121. ASME BPVC Code Case N-643, Fatigue Crack Growth Rate Curves for Ferritic Steels in PWR Water Environment, Section XI, Division 1. In: *ASME Boiler and Pressure Vessel Code.* New York: American Society of Mechanical Engineers.

122. Seifert HP, Ritter S. Effect of Temperature and Loading Frequency on SICC and Corrosion Fatigue Crack Growth Behavior of Low-Alloy RPV Steels Under BWR/NWC Conditions. Eleventh International Conference on Environmental Degradation of Materials in Nuclear Power Systems – Water Reactors, 2003.

123. Ford FP, Andresen PL. Development and Use of a Predictive Model of Crack Propagation in 304/316L, A533B/A508 and Inconel 600/182 Alloys in 288¡C Water. Proceedings of Third International Symposium on Environmental Degradation of Materials in Nuclear Power Systems -Water Reactors, TMS-AIME, Warrendale, 1988, pp. 789–800.

124. Carter, R. and Pathania, R., “Technical Basis for BWRVIP Stainless Steel Crack growth Correlations in BWRs.” Proceedings of ASME PVP 2007, Paper # PVP2007-26618.

125. Mehta HS. Fatigue and SCC Growth Rate Relationships for Austenitic and Nickel-Based Materials in BWR Water Environment – A BWRVIP and GE Perspective. Proceedings of Workshop on Flaw Growth in Austenitic and Nickel-Based Materials, August 1, 2002, Snowbird, Utah.

126. U.S. NRC Final Safety Evaluation Report on BWRVIP-14 (TAC M94975). Washington, DC: U.S. Nuclear Regulatory Commission; 1999.

127. Andresen PL. Fracture Mechanics Data and Modeling of Environmental Cracking of Nickel-Base Alloys in High Temperature Water, Paper No. 44, Corrosion 91, Cincinnati, Ohio, March 11–15, 1991.

128. Ford FP, et al. Stress Corrosion Cracking of Low Alloy Steels Under BWR Conditions; Assessment of Crack Growth Rate Algorithms. Proceedings of Ninth International Symposium on Environmental Degradation of Materials in Nuclear Power Systems – Water Reactors, 1999, pp. 855–864.

129. Evaluation of Reactor Pressure Vessel Head Cracking in Two Domestic BWRs (EPRI Report TR-101971). Palo Alto, CA: Electric Power Research Institute; 1993.

130. Kiss E, Ranganath S. On-Line Monitoring to Assure Structural Integrity of Nuclear Reactor Components. *International Journal of Pressure Vessel and Piping* 1988;34:3–15.